Received: 25 March 2020 | Revised: 16 June 2020 | Accepted: 30 July 2020

DOI: 10.1111/gbi.12412

ORIGINAL ARTICLE

gebiology WILEY

Understanding the geobiology of the terminal Ediacaran Khatyspyt Lagerstätte (Arctic Siberia, Russia)

Jan-Peter Duda[1,2] | Gordon D. Love[1] | Vladimir I. Rogov[3] | Dmitry S. Melnik[3,4] | Martin Blumenberg[5] | Dmitriy V. Grazhdankin[3,4]

[1]Department of Earth and Planetary Sciences, University of California, Riverside, CA, USA

[2]Geobiology Group, Geoscience Centre, University of Göttingen, Göttingen, Germany

[3]Trofimuk Institute of Petroleum Geology and Geophysics, Siberian Branch Russian Academy of Sciences, Novosibirsk, Russia

[4]Novosibirsk State University, Novosibirsk, Russia

[5]Federal Institute for Geosciences and Natural Resources (BGR), Hannover, Germany

Correspondence
Jan-Peter Duda, Geobiology Group, Geoscience Center, University of Göttingen, Goldschmidtstr. 3, 37077 Göttingen, Germany.
Email: jduda@gwdg.de

Funding information
Financial support was obtained by the following: German Research Foundation (DFG; research fellowship DU 1450/4-1, project DU 1450/5-1) (JPD); Research Department of the University of Göttingen (JPD); Field work was supported by the Russian Foundation for Basic Research (grant 18-05-70110); Russian Science Foundation (grant 20-67-46028) (VIG, DSM, DVG).

Abstract

The Khatyspyt Lagerstätte (~544 Ma, Russia) provides a valuable window into late Ediacaran Avalon-type ecosystems with rangeomorphs, arboreomorphs, and mega-algae. Here, we tackle the geobiology of this Lagerstätte by the combined analysis of paleontological features, sedimentary facies, and lipid biomarkers. The Khatyspyt Formation was deposited in carbonate ramp environments. Organic matter (0.12–2.22 wt.% TOC) displays characteristic Ediacaran biomarker features (e.g., eukaryotic steranes dominated by the C_{29} stigmastane). Some samples contain a putative 2-methylgammacerane that was likely sourced by ciliates and/or bacteria. 24-isopropylcholestane and 26-methylstigmastane are consistently scarce (≤0.4% and ≤0.2% of $\sum C_{27\text{-}30}$ regular steranes, respectively). Thus, Avalon-type organisms occupied different niches than organisms capable of directly synthesizing C_{30} sterane precursors among their major lipids. Relative abundances of eukaryotic steranes and bacterial hopanes (sterane/hopane ratios = 0.07–0.30) demonstrate oligotrophic and bacterially dominated marine environments, similar to findings from other successions with Ediacara-type fossils. Ediacara-type fossils occur in facies characterized by microbial mats and biomarkers indicative for a stratified marine environment with normal–moderate salinities (moderate–high gammacerane index of 2.3–5.7; low C_{35} homohopane index of 0.1–0.2). Mega-algae, in contrast, are abundant in facies that almost entirely consist of allochthonous event layers. Biomarkers in these samples indicate a non-stratified marine environment and normal salinities (low gammacerane index of 0.6–0.8; low C_{35} homohopane index of 0.1). Vertical burrowers occur in similar facies but with biomarker evidence for stratification in the water column or around the seafloor (high gammacerane index of 5.6). Thus, the distribution of macro-organisms and burrowers was controlled by various, dynamically changing environmental factors. It appears likely that dynamic settings like the Khatyspyt Lagerstätte provided metabolic challenges for sustenance and growth which primed eukaryotic organisms to cope with changing environmental habitats, allowing for a later diversification and expansion of complex macroscopic life in the marine realm.

KEYWORDS
ichnofabrics, lipid biomarkers, methylgammacerane, methylgammacerane index (MGI), sedimentary facies, trace fossils, vertical bioturbation

1 | INTRODUCTION

The Ediacaran (*ca*. 635–541 million years, Ma) records the diversification of complex macroscopic life on our planet (best exemplified by "Ediacara-type organisms"), which heralded one of the most fundamental geobiological transitions in Earth's history (Knoll, Walter, Narbonne, & Christie-Blick, 2004, 2006; Narbonne, 2005; Narbonne, Xiao, Shields, & Gehling, 2012; Xiao & Laflamme, 2009). The biological affinity of Ediacara-type organisms is still puzzling, but some forms might represent early metazoans (e.g., Fedonkin, 1990; Gehling, 1991; Glaessner, 1984). Furthermore, still little is known about the geobiology of the host ecosystems, that is, including microbial communities and environmental conditions. This is because fossils of Ediacara-type organisms are usually preserved as imprints in siliciclastic or volcaniclastic facies (e.g., Narbonne, 2005), resulting in a significant loss of textural and biogeochemical information (Duda, 2014; Duda, Blumenberg, et al., 2014; Duda, Thiel, et al., 2014; Duda, Thiel, Reitner, & Grazhdankin, 2016; Grazhdankin, Balthasar, Nagovitsin, & Kochnev, 2008). Carbonate records such as the Khatyspyt Formation (*ca*. 544 Ma, Arctic Siberia) provide complementary taphonomic windows and may give important insights into prevailing ecological baseline conditions.

The Khatyspyt Formation has been attracting much attention as it contains a great diversity of Ediacara-type fossils (Avalon-type assemblage including rangeomorphs and arboreomorphs), carbonaceous compression fossils (informally grouped as "*mega-algae*" *sensu* Steiner, Erdtmann, & Chen, 1992), and trace fossils (Bykova, Gill, Grazhdankin, Rogov, & Xiao, 2017; Fedonkin, 1990; Grazhdankin et al., 2008; Nagovitsin et al., 2015; Rogov et al., 2012; Sokolov & Fedonkin, 1984; Vodanjuk, 1989). Because of the exceptional preservation of fossils from the macro to the molecular scale (i.e., organic biomarkers), it has been considered a fossil lagerstätte *sensu* Seilacher (1970) (Duda et al., 2016). Interestingly, distinct body and trace fossil associations occur in different sedimentary facies, possibly indicating biological responses to shifting environmental conditions. Indeed, preliminary biomarker data and inorganic geochemical proxies (e.g., stable carbon and sulfur isotopes) hint at a relation between paleo-redox conditions and macrofossil occurrences (Cui et al., 2016; Duda et al., 2016, 2019; Melnik, Parfenova, Grazhdankin, & Rogov, 2019). Detailed analyses of organic biomarker assemblages in different facies of the Khatyspyt Formation can help to assess environmental controls on biological variability in this unique fossil lagerstätte further.

This study tackles the geobiology of the Khatyspyt Lagerstätte by combining detailed paleontological and sedimentological observations with systematic organic biomarker analyses of different facies. This integrative approach taps the full geobiological potential of the Khatyspyt record, providing valuable insights into ecosystem functioning at this critical transition of Earth's history. We will reconstruct biological communities and environmental conditions in the Khatyspyt Lagerstätte and test potential controls on the distribution of Avalon-type macro-organisms and mega-algae. Furthermore, we will discuss our results in the light of findings from other Ediacaran marine ecosystems (e.g., Oman, Baltica, South China).

2 | GEOLOGICAL SETTING

The Khatyspyt Formation crops out along the Khorbusuonka River which cuts through the north-western slope of the Olenek Uplift on the northeastern Siberian Platform (Arctic Russia). It rests on the Maastakh Formation and is overlaid by the Turkut Formation, all of which belong to the terminal Ediacaran Khorbusuonka Group (Figure 1). Detailed accounts on the local geology and stratigraphy are provided elsewhere (e.g., Grazhdankin, Marusin, et al., 2020; Grazhdankin, Nagovitsin, et al., 2020; Knoll, Grotzinger, Kaufman, & Kolosov, 1995; Nagovitsin et al., 2015; Pelechaty, Grotzinger, Kashirtsev, & Zhernovsky, 1996; Pelechaty, Kaufman, & Grotzinger, 1996; Rogov et al., 2015).

The Khatyspyt Formation is laterally not extensive and typically less than 190 m thick (Nagovitsin et al., 2015; Pelechaty, Grotzinger, et al., 1996; Pelechaty, Kaufman, et al., 1996). It can be subdivided into four members mainly comprising limestones (partly dolomitized) and shales (Nagovitsin et al., 2015) (Figure 1). In the type area, sedimentary facies indicates deposition in low-energy carbonate ramp environments below storm wave base (Knoll et al., 1995; Nagovitsin et al., 2015). To the east and southwest, however, limestone beds exhibiting hummocky cross-stratification become more abundant and progressively thicker (e.g., Berkekit River, Kersyuke River, upper Khorbusuonka River, Kyutingde River basin), suggesting higher hydrodynamic energies (Nagovitsin et al., 2015). Further to the south, the Khatyspyt Formation correlates with thick-bedded limestones and dolomites (Kyutingde River basin, Ulakhan-Uettyakh and Balagannakh tributaries) (Nagovitsin et al., 2015). Thus, environments to the east and southwest were likely slightly shallower than in the type area, and the depositional system deepened gradually to the northwest. The overlying Turkut Formation consists of evaporitic carbonates (Knoll et al., 1995; Nagovitsin et al., 2015; Pelechaty, Grotzinger, et al., 1996; Yakshin, 1987).

Because of the presence of ubiquitous organic matter, it was inferred that the Khatyspyt Formation was deposited under anoxic conditions beneath a stratified water column (Knoll et al., 1995; Pelechaty, Kaufman, et al., 1996). Indeed, stable carbon and sulfur isotopes suggest the initial presence of a stratified water body with episodes of euxinic deeper water that shifted to non-euxinic conditions (Cui et al., 2016). This is fairly similar to the Shibantan Member in South China (Duda, 2014; Duda, Blumenberg, et al., 2014; Duda, Zhu, & Reitner, 2015) and, possibly, parts of the Ara Group in south Oman (see Schröder & Grotzinger, 2007).

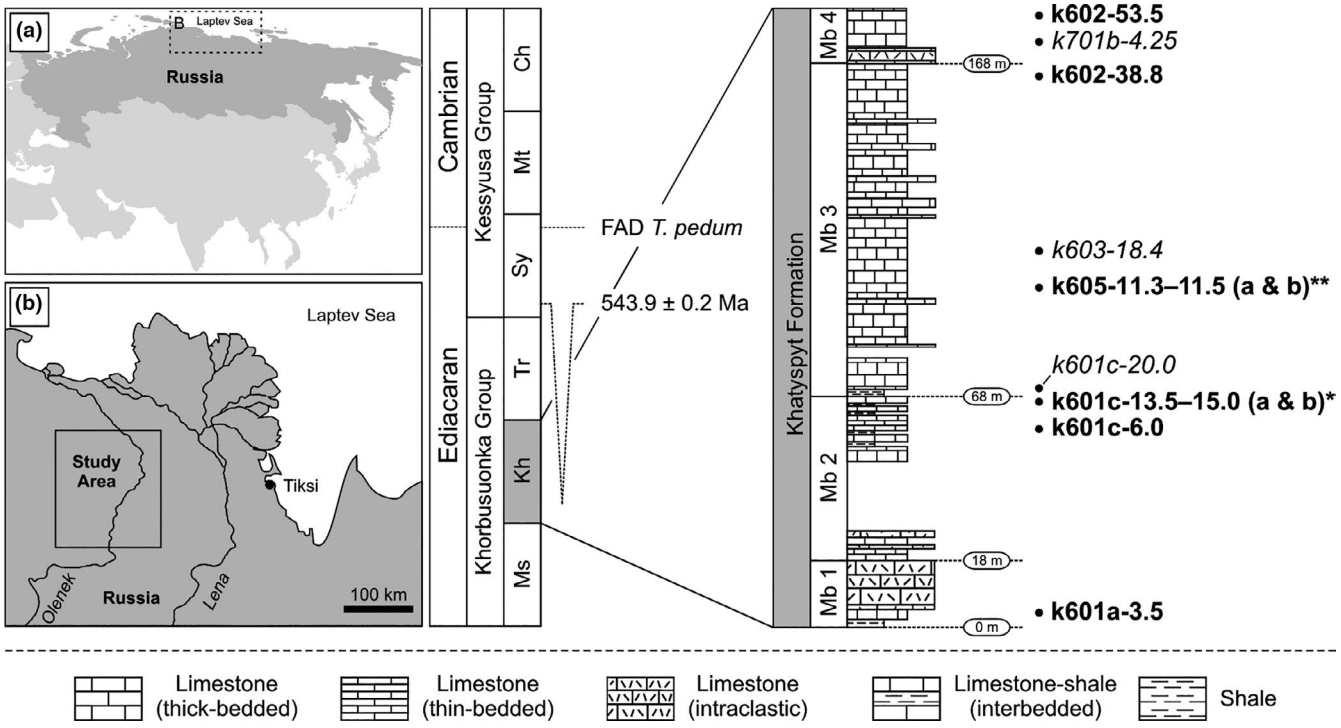

FIGURE 1 Working area and composite section of the Khatyspyt Formation (modified after Nagovitsin et al., 2015, Rogov et al., 2015; U-Pb zircon age of 543.9 ± 0.2 Ma from Bowring et al., 1993). Please note that the sample positions are only approximate and not to scale. Samples in bold were analyzed for organic biomarkers. Ch, Chuskuna Formation; Kh, Khatyspyt Formation; Ms, Maastakh Formation; Mt, Mattaia Formation; Sy, Syhargalakh Formation; Tr, Turkut Formation. FAD, First appearance datum. Asterisks mark samples from intervals with abundant and well-preserved fossils of Ediacara-type organisms (*) and mega-algae (**)

The Khatyspyt Formation, together with the overlying Turkut and Syhargalakh formations, is locally intruded by diatremes that exhibit a U-Pb zircon age of 543.9 ± 0.2 Ma (Bowring et al., 1993; Knoll et al., 1995; Nagovitsin et al., 2015; Rogov et al., 2015) (Figure 1). The Turkut Formation contains internal molds of various tubular fossils of uncertain affinity, possibly including poorly preserved cloudinids and/or *Cambrotubulus decurvatus* (Khomentovsky & Karlova, 1993; Rogov et al., 2015). The current index fossil for the Ediacaran–Cambrian boundary (*Treptichnus pedum*: Brasier, Cowie, & Taylor, 1994; Landing, 1994; Markov, Rogov, Karlova, & Grazhdankin, 2019) first appears in the uppermost Syhargalakh Formation (Grazhdankin, Marusin, et al., 2020; Grazhdankin, Nagovitsin, et al., 2020; Nagovitsin et al., 2015). The Khatyspyt Formation is thus of uppermost Ediacaran age (*ca.* 544 Ma) (Nagovitsin et al., 2015; Rogov et al., 2015), which is further supported by chemostratigraphic correlation (Cui et al., 2016, 2019).

3 | MATERIAL AND METHODS

3.1 | Petrography and bulk analyses

The analyzed samples were stored in collections of the Trofimuk Institute of Petroleum Geology and Geophysics, Siberian Branch of the Russian Academy of Sciences (Novosibirsk, Russia). Thin sections (vertical cross sections) were prepared for all samples. Petrographic observation of thin sections (transmitted and reflected light) was conducted with a Zeiss SteREO Discovery.V8 stereomicroscope linked to an AxioCam MRc5 5-megapixel camera.

Contents of total organic carbon (TOC), sulfur (S_{tot}), and nitrogen (N_{tot}) were determined with a Hekatech Euro EA elemental analyzer and a Leco RC612 temperature programmable carbon analyzer. All values are reported in weight % (wt.%) of bulk sedimentary rock.

Rock-Eval pyrolysis was performed on unextracted sample powders with a Rock-Eval 6 instrument following the method described by Espitalié et al. (1977). Briefly, the temperature was ramped from 300°C (held for 3 min) to 650°C at 25°C/min. Pyrolysis products and released CO_2 were analyzed with a flame ionization detector (FID) and an infrared cell, respectively. The measurements included quantities of free hydrocarbons (S1, mg HC/g rock) and hydrocarbons yielded from the labile kerogen (S2, mg HC/g rock), temperatures at maximum yields of S2 hydrocarbons (T_{max}, °C), as well as the CO_2 generated from organic carbon at higher temperature up to 650°C (S3, mg CO_2/g rock). All these data were used to calculate the hydrogen index (HI; S2/TOC * 100), oxygen index (OI; S3/TOC * 100), and production index (PI; S1/(S1 + S2)) for each sample.

3.2 | Sample preparation for organic biomarker analysis

Selected samples of different Khatyspyt facies were analyzed for lipid biomarkers using established methodology (Duda, 2014;

Duda, Blumenberg, et al., 2014; Duda, Thiel, et al., 2014; Duda et al., 2016) (Figure 1). All glassware and other laboratory materials were heated to 500°C for 3 hr and/or extensively rinsed with acetone to circumvent trace organic contamination transfer to rocks and rock powders. Full procedural blanks (pre-combusted sea sand) were prepared and analyzed in parallel to monitor laboratory contaminations.

Exterior parts of all samples (≥5 mm) were removed with a pre-cleaned precision saw (Buehler IsoMet 1000). The exterior and interior parts were then crushed and powdered using a pebble mill (Retsch MM 301). Ground sample material (*ca*. 20 g) was extracted in the following steps: (a) dichloromethane (DCM), (b) DCM/*n*-hexane (1/1; *v*/*v*), and (c) *n*-hexane (20 min ultrasonication, respectively). The resulting extracts were combined, desulfurized with activated copper, and gently concentrated using a pre-cleaned rotary evaporator and N_2 to avoid a major loss of low-boiling compounds (Ahmed & George, 2004). The isolates were then fractionated by column chromatography (1.5 cm in diameter, 8 cm in height; 7 g of dry silica gel). The saturated fraction (F1) was eluted with *n*-hexane (27 ml), the aromatic fraction (F2) with *n*-hexane/DCM (1/1; *v*/*v*; 32 ml), and a polar residue (F3) with DCM/MeOH (1/1; *v*/*v*; 40 ml).

Our results reported are for the interior rock portions which are much less prone to containing contaminant contributions. Comparisons between outer and inner portions were performed (Figure S1) and showed very similar compound profiles and negligible contamination of outer portions in all cases.

3.3 | Gas chromatography–mass spectrometry

Gas chromatography–mass spectrometry (GC–MS) analyses were carried out with a Thermo Scientific Trace 1300 Series GC coupled to a Thermo Scientific Quantum XLS Ultra MS. The GC was equipped with a Phenomenex Zebron ZB-5 column (30 m length, 0.25 mm inner diameter, 0.25 μm film thickness). Saturated and aromatic fractions were injected into a splitless injector and transferred to the GC column at 300°C. Helium was used as carrier gas with a flow rate of 1.5 ml/min. The GC oven temperature was ramped from 80°C (held for 1 min) to 310°C (held for 20 min) at 5°C/min. Electron ionization mass spectra were recorded in full-scan mode at an electron energy of 70 eV with a mass range of *m*/*z* 50–600 and scan time of 0.42 s.

3.4 | Metastable reaction monitoring–gas chromatography–mass spectrometry

Metastable reaction monitoring–gas chromatography–mass spectrometry (MRM–GC–MS) was conducted on a Waters Autospec Premier MS coupled to an Agilent 7890A GC. The GC was equipped with a DB-1MS column (60 m length, 0.25 mm inner diameter, 0.25 μm film thickness). 1–2 μl of the saturated hydrocarbon fractions dissolved in *n*-hexane were injected onto the GC column in splitless injection mode and transferred to the GC column at 320°C. Helium was used as carrier gas with a flow rate of 1.0 ml/min. The GC oven temperature was ramped from 60°C (held for 2 min) to 150°C at 10°C/min and then to 320°C at 3°C/min (held for 22.5 min). Analyses were performed in electron impact (EI) mode with an ionization energy of 70 eV and an accelerating voltage of 8 kV. The analysis included MRM transitions for tricyclic terpanes (C_{19}–C_{26}), tetracyclic terpanes (C_{24}), steranes (C_{21}–C_{22} and C_{26}–C_{30}), methylsteranes (C_{30}), hopanes (C_{27}–C_{35}), and methylhopanes (C_{31}–C_{36}).

3.5 | Calculated biomarker indices

Carbon preference indexes (CPI) for *n*-alkanes, as well as triterpane- and sterane-based indices, were calculated from full-scan GC–MS by integrating peak areas in partial mass chromatograms (*m*/*z* 85, 191, and 217, respectively) following established formulae (Bray & Evans, 1961; Killops & Killops, 2005; Mello et al., 1988; Peters, Walters, & Moldowan, 2005; Seifert & Moldowan, 1978, 1980, 1986). The only MRM–GC–MS data-based indices are relative abundances of regular C_{27}–C_{29} steranes (C_{27}, C_{28}, and C_{29} sterane channels, respectively), relative C_{30} sterane abundances (summed C_{27}–C_{30} sterane channels), and a newly proposed methylgammacerane index (MGI; 412 → 191 and 426 → 205 Da ion transitions for gammacerane and methylgammacerane, respectively). CPIs were calculated as $0.5 * [(C_{25}–C_{33})_{odd}/(C_{24}–C_{32})_{even} + (C_{25}–C_{33})_{odd}/(C_{26}–C_{34})_{even}]$ (Bray & Evans, 1961). C_{35} homohopane indexes were calculated as the ratio $C_{35}/(C_{31}–C_{35})$ homohopanes. Gammacerane indexes (GI) and MGI were calculated using the formulas 10 * gammacerane/(gammacerane + C_{30} αβ hopane) (after Peters et al., 2005) and 10 * methylgammacerane/(methylgammacerane + gammacerane).

Polyaromatic hydrocarbon (PAH) parameters were calculated from full-scan GC–MS based on phenanthrene (P) and methylphenanthrenes (MP) using *m*/*z* 178 and 192 fragmentograms, respectively. The methylphenanthrene index (MPI-1) was calculated as 1.5 * (2MP + 3MP)/(P + 1MP + 9MP) (Radke & Welte, 1983; Radtke, Welte, & Willsch, 1982). Equivalent vitrinite reflectance (R_c) was calculated from MPI-1 values using the formula 0.7 * MPI-1 + 0.22 since P/MP ratios are <1 for all samples (Boreham, Crick, & Powell, 1988) (Table 1). Methylphenanthrene ratios (MPR) were calculated as 2MP/1MP (Radke, Welte, & Willsch, 1986).

Formulae for all other molecular indices are provided in the text.

4 | RESULTS

4.1 | Petrographic features

The Khatyspyt Formation comprises finely laminated bituminous limestones, marls, and shales (Figure 1). Most of the observed samples contain abundant μm-sized pyrite crystals.

Fossils of macroscopic, complex organisms are most abundant and best preserved in two distinct stratigraphic intervals (Figure 1,

TABLE 1 Maturity-sensitive aliphatic and aromatic biomarker hydrocarbon ratios

Sample ID	CPI	C_{31} hopane 22S/(22S + 22R)	Ts/(Ts + Tm)	C_{29} sterane 20S/(20S + 20R)	C_{29} sterane ββ/(ββ + αα)	MPI-1	P/MP	R_c(MPI-1)	MPR
k602-53.5	0.99	0.57	0.30	0.50	0.42	0.43	0.72	0.52	0.93
k602-38.8	1.02	0.59	0.28	0.48	0.46	0.65	0.36	0.68	1.23
k605-11.3–11.5a	1.14	0.59	0.34	0.49	0.34	0.31	0.99	0.44	0.89
k605-11.3–11.5b	1.16	0.59	0.35	0.47	0.30	0.32	0.94	0.45	0.89
k601c-13.5–15.0a	0.99	0.58	0.27	0.52	0.46	0.52	0.80	0.58	1.45
k601c-13.5–15.0b	1.07	0.57	0.28	0.47	0.55	0.49	0.60	0.57	0.89
k601c-6.0	(1.02)	(0.62)	(0.45)	(0.51)	(0.53)	(0.31)	(0.91)	(0.44)	(0.72)
k601a-3.5	1.00	0.60	0.37	0.51	0.51	0.45	0.41	0.53	0.75

Note: The presented data suggest early oil window maturity levels of organic matter, substantially prior to peak oil generation. Please note that lipid biomarker data cannot be considered absolutely valid for sample k601c-6.0.

Abbreviations: C_{31} hopane isomers, 17α(H),21β(H) 22S + 22R; C_{29} sterane isomers, 5α(H),14α(H),17α(H) 20S + 20R, 5α(H),14β(H),17β(H) 20R + 20S; CPI, carbon preference index, calculated as $0.5*[(C_{25}–C_{33})_{odd}/(C_{24}–C_{32})_{even} + (C_{25}–C_{33})_{odd}/(C_{26}–C_{34})_{even}]$ (Bray & Evans, 1961); MP, methylphenanthrenes; MPI-1, methylphenanthrene index, calculated as 1.5*(2MP + 3MP)/(P + 1MP + 9MP) (Radke & Welte, 1983; Radtke et al., 1982); MPR, methylphenanthrene ratios, calculated as 2MP/1MP (Radke et al., 1986); P, phenanthrene; R_c (MPI-1), Vvitrinite reflectance calculated from MPI-1 values as 0.7*MPI-1 + 0.22 since P/MP ratios are <1 for all samples (Boreham et al., 1988); Ts and Tm, 22,29,30-trisnorhopanes (C_{27}).

Table 2). Mega-algae assemblages tend to occur in laminated limestones consisting of an alternation of thin (<1 mm) micritic to fine-grained calcite layers (k605-11.3–11.5a,b; Figure 2a). Fossils of Ediacara-type organisms, in contrast, are preserved in facies that additionally exhibit interwoven networks of very thin, dark-brownish laminae (k601c-13.5–15.0a,b; Figure 2b). Notably, some of the samples from this interval are recrystallized to an extent that any other primary features such as grains are lost (k601c-13.5–15.0b; Figure 2c).

In samples from other parts of the Khatyspyt Formation, primary sedimentary features such as the original bedding and lamination appear to be disturbed (e.g., k701b-4.25; Figure 2d). In addition, the formation comprises bituminous limestones that are not laminated on the microfacies scale (e.g., k601c-6.0; Figure 2e). Grainy layers in undisturbed and well-preserved facies commonly exhibit sparry calcite cements (Figure 2f). These cements are very prominent and can even be recognized in hand specimens by the unaided eye.

In cross section, samples from the interval with Ediacara-type fossils locally comprise small (<1 mm) circular to oval structures that are filled with grains or carbonate cements (k601c-13.5–15.0a; Figure 3a). These structures are oriented parallel to bedding and typically less compacted than the surrounding layers. Some samples from the top of the sections also exhibit structures that extend vertically (k602-38.8, k701b-4.25). In case of well-layered samples, these structures display distinct fishhook- and antler-like shapes (Figure 3b,c). Structures in samples with disturbed bedding are not as distinctly shaped and filled with small sparite cements (Figure 2d). Notably, these structures are typically associated with mottled fabrics (Figure 3d).

Some samples from the Khatyspyt Formation contain small (<380 μm) components of various shapes (Figure S2). Some of these might be remains of shelly organisms, but this requires further investigation. Therefore, the components are classified as *incertae sedis*.

4.2 | Organic geochemistry—bulk characteristics

Bulk sedimentary organic matter data are listed in Table 3. TOC contents of the analyzed samples range from very low to high values (0.12–2.22 wt.%). Sulfur and nitrogen contents are low (0.01–0.08 and 0.01–0.04 wt.%, respectively). Rock-Eval data are only considered totally robust here if TOC contents are ≥0.2 wt.% and S2 values are >0.5 mg HC/g rock (see Peters, 1986; Peters & Cassa, 1994). Robust T_{max} values range between 429 and 437°C. PI values range between 0.02 and 0.34. HI and OI values show a wide range of variation (162–419 mg HC/g TOC and 19–105 mg CO_2/g TOC, respectively). There is no obvious stratigraphic trend to the organic geochemical bulk data. The chromatograms exhibit no appreciable hump of an unresolved complex mixture of organic compounds (UCM) (Figure 4).

4.3 | Organic biomarker inventories

4.3.1 | Linear and branched alkanes

A series of *n*-alkanes is detected, mostly in the range from C_{12} to C_{38} (Figure 4). Most samples show no strong carbon number predominance, but few have distinct maxima at C_{17} and C_{19} (e.g., k605-11.3–11.5a; Figure 4). $CPI_{24–34}$ values are generally consistent (0.99–1.16; Table 1). Terminally methyl-branched alkanes (*iso*- and *anteiso*isomers) are present in all analyzed samples, with chain lengths typically ranging from C_{13} (i.e., methyl-C_{12}) to C_{27} (i.e., methyl-C_{26}). Mid-chain methyl-branched alkanes including X-peaks (C_{14}–C_{30}, with greatest abundance between C_{20} and C_{26}; Love, Stalvies, Grosjean, Meredith, & Snape, 2008) are only present in traces. Cyclohexylalkanes are prominent compounds in all samples where they usually range from C_{12} to C_{26} and show no carbon number preferences (Figure 4).

TABLE 2 Sedimentary facies characteristics and source and environment-sensitive biomarker ratios

Sample ID	Facies characteristics		Lipid biomarkers							
			Ster/hop ratio	% C_n steranes			C_{35}-HHI	GI	MGI	
ID	Sedimentology	Paleontology		C_{27}	C_{28}	C_{29}	C_{35}/(C_{31}–C_{35})	10*G/(G + C_{30}hop)	10*MG/(MG + G)	Environ. conditions
k602-53.5	Event deposits + microbial mats	–	0.10	23	15	62	0.2	4.9	2.0	Stratified water body, normal–moderate salinities
K701b-4.25	Event deposits	Vertical burrowers	–	–	–	–	–	–	–	–
k602-38.8			0.10	21	13	66	0.2	5.6	2.2	Stratified water body, normal–moderate salinities
K603-18.4		–	–	–	–	–	–	–	–	–
k605-11.3–11.5a		Mega-algae fossils	0.30	18	11	71	0.1	0.6	5.6	Non-stratified water body, normal salinities
k605 11.3–11.5b			0.30	17	10	73	0.1	0.8	4.5	
K601c-20.0		–	–	–	–	–	–	–	–	–
k601c-13.5–15.0a	Microbial mats	Ediacara-type fossils, horizontal traces	0.17	22	14	65	0.2	5.7	3.6	Stratified water body, normal–moderate salinities
k601c-13.5–15.0b			0.19	20	9	71	0.1	2.3	1.7	
k601c-6.0	No bedding/lamination	–	(0.12)	(19)	(16)	(65)	(0.4)	(4.3)	(2.5)	
k601a-3.5	Event deposits	–	0.07	22	11	67	0.2	3.2	2.0	

Note: The C_{35} homohopane, gammacerane, and methylgammacerane indexes (HHI, GI, and MGI, respectively) show a wide range of values, reflecting dynamically changing marine environmental conditions in the Khatyspyt Lagerstätte (e.g., water column stratification). Samples in italics were not analyzed for organic biomarkers. Please also note that lipid biomarker data cannot be considered absolutely valid for sample k601c-6.0. The GI was calculated after Peters et al. (2005).

G, gammacerane; MG, methylgammacerane.

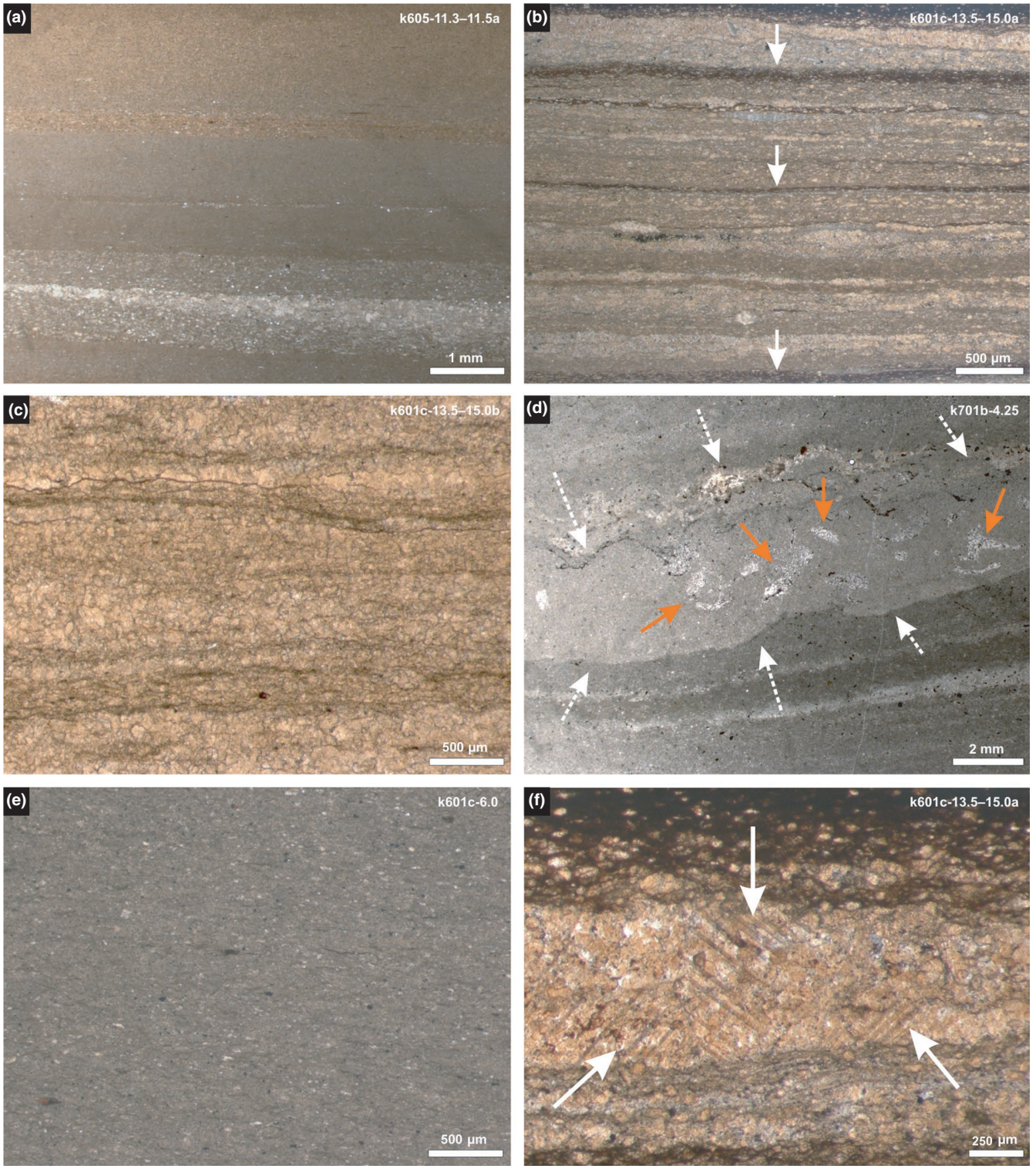

FIGURE 2 Thin section photographs of selected Khatyspyt facies (cross sections). (a, b) Finely laminated bituminous limestones and marls. The lamination is due to an alternation of thin (<1 mm) micritic to fine-grained layers (a, b) and, additionally, to microbial lamination and pressure solution seams (examples marked by arrows in b). Fossils of Ediacara-type organisms and mega-algae are preserved in these facies. (c) Laminated but recrystallized bituminous limestone. Note that primary features such as grains are lost. (d) Limestone facies with disturbed bedding (dashed white arrows) and sparitic structures (continuous orange arrows). The same facies also exhibit mottled fabrics (Figure 3d). All these features are typical traits of ichnofabrics that were produced by vertical burrowers. (e) Bituminous limestone that is not laminated on the microfacies scale. (f) Sparry calcite overgrowth cements in a grainy layer (arrows). These cements are widespread in the Khatyspyt Formation and can even be recognized in hand specimens by the unaided eye. Note also microbial laminae that interweave sedimentary grains at the top of the photo

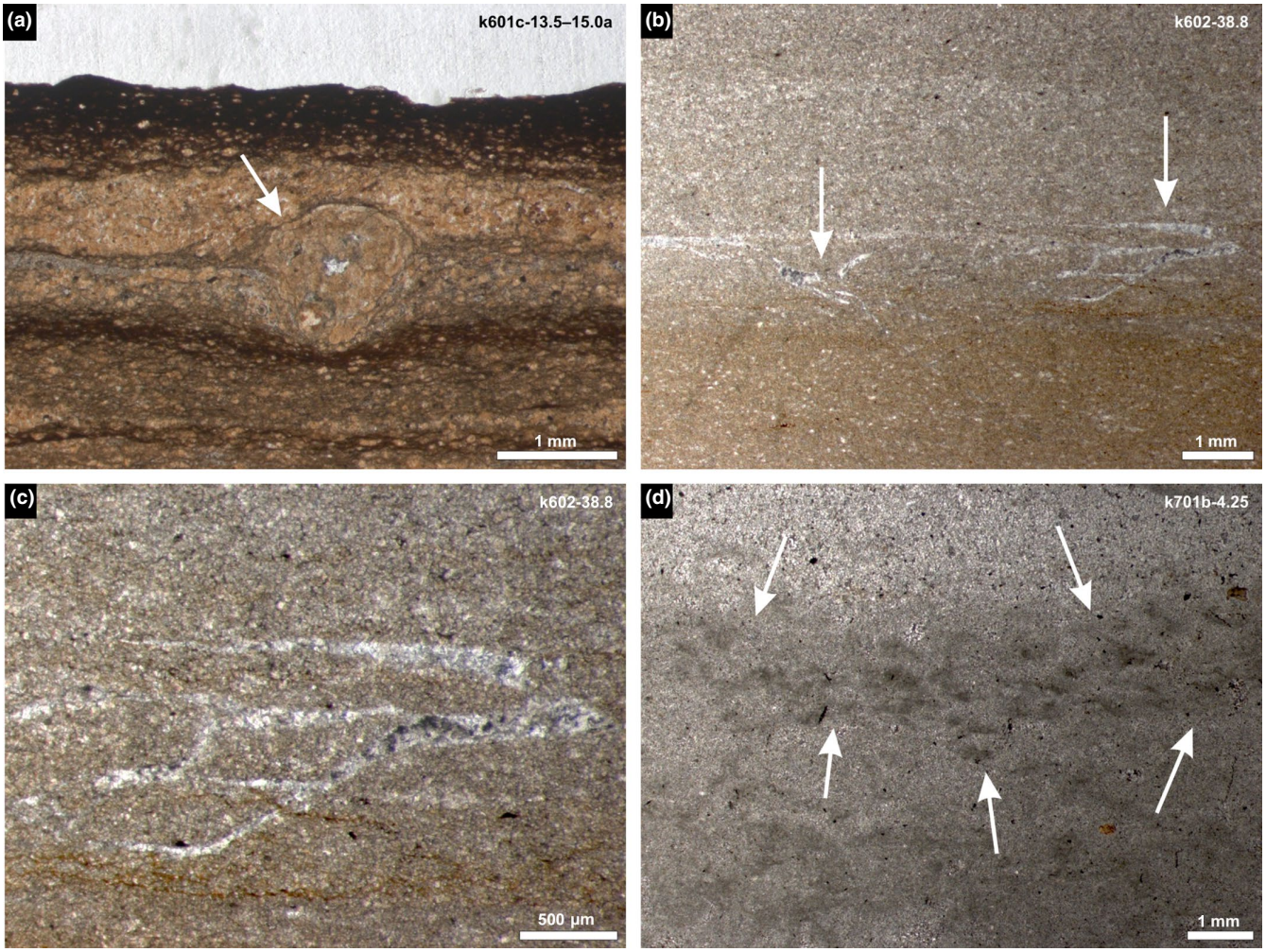

FIGURE 3 Thin section photographs of selected Khatyspyt ichnofabrics (cross sections). (a) Circular to oval structures filled with carbonate cement (arrow) interpreted as horizontal burrow. (b, c) Structures with fishhook- and antler-like shapes (arrows) interpreted as vertical burrows (c is a close up of b). (d) Mottled fabrics (arrows) occurring in limestone facies that exhibits disturbed bedding as well as sites of selective replacement and preferential cementation (Figure 2d). These features are typically produced by vertical burrowers, as commonly observed in Phanerozoic carbonates

TABLE 3 Total organic carbon (TOC) contents and Rock-Eval pyrolysis parameters (non-robust Rock-Eval data in italics)

Sample ID	TOC (wt.%)	S_{tot} (mean wt.%)	N_{tot} (mean wt.%)	T_{max} (°C)	S1 (mg HC/g rock)	S2 (mg HC/g rock)	S3 (mg CO_2/g rock)	PI (S1/(S1 + S2))	HI (mg HC/g TOC)	OI (mg CO_2/g TOC)
k602-53.5	0.59	0.01	0.02	432	0.04	1.92	0.29	0.02	325	49
k602-38.8	0.20	0.01	0.01	*442*	*0.02*	*0.30*	*0.25*	*0.06*	*150*	*125*
k605-11.3–11.5a	0.42	0.05	0.02	432	0.11	1.54	0.18	0.07	367	43
k605 11.3–11.5b	0.74	0.02	0.02	431	0.10	1.87	0.78	0.05	253	105
k601c-13.5–15.0a	2.22	0.08	0.04	429	0.82	9.31	0.42	0.08	419	19
k601c-13.5–15.0b	0.15	0.06	0.01	*445*	*0.05*	*0.27*	*0.24*	*0.16*	*180*	*160*
k601c-6.0	0.39	0.03	0.02	437	0.32	0.63	0.36	0.34	162	92
k601a-3.5	0.12	0.02	0.01	*428*	*0.01*	*0.13*	*0.11*	*0.07*	*108*	*92*

Abbreviations: HC, hydrocarbons; HI, hydrogen index, calculated as S2/TOC * 100; OI, oxygen index, calculated as S3/TOC * 100; PI, production index, calculated as S1/(S1 + S2); S1, measured quantities of free hydrocarbons; S2, measured quantities of hydrocarbons yielded from the kerogen; S3, measured quantities of CO_2 generated from organic carbon up to 650°C.

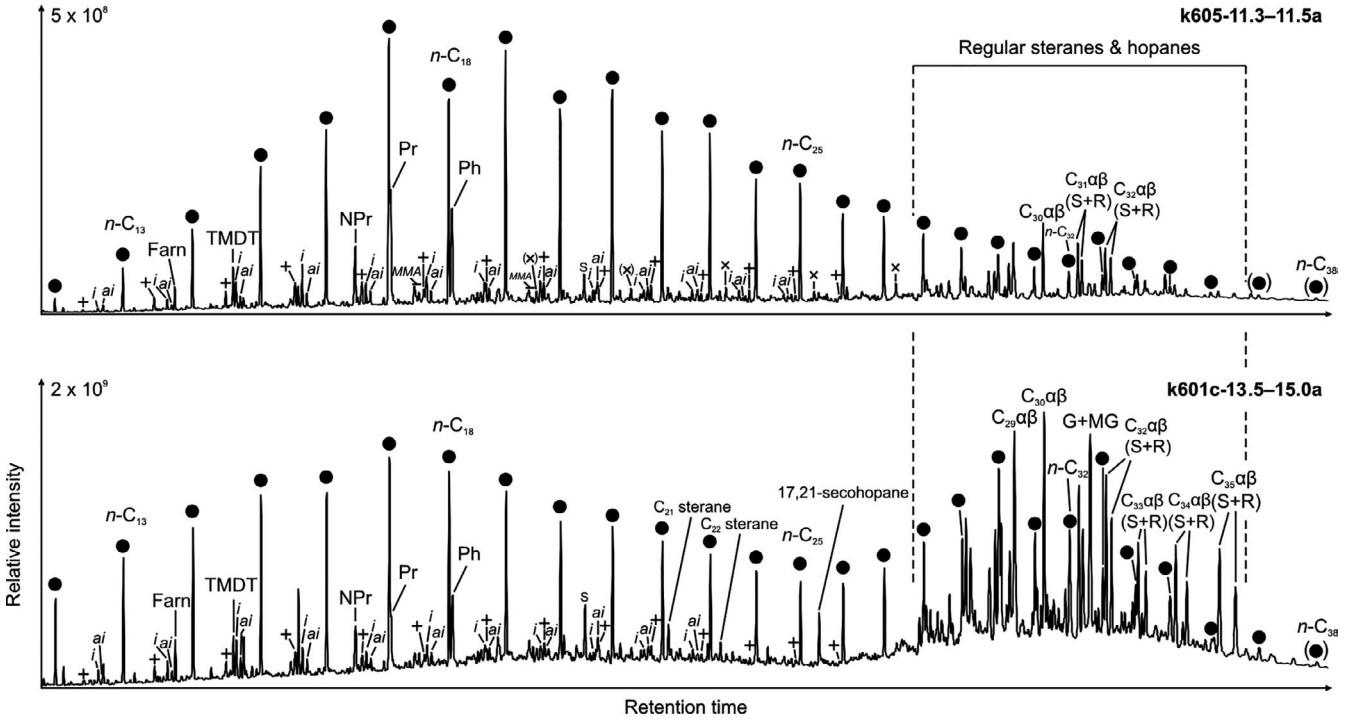

FIGURE 4 Full-scan chromatograms (total ion current; TIC) of saturated hydrocarbon fractions. Note that all runs lack a hump of an unresolved complex mixture (UCM). Black circles: *n*-alkanes; Regular crosses: cyclohexylalkanes; *i*: *iso*-alkanes; *ai*: *anteiso*-alkanes; Farn: Farnesane; TMDT: 2,6,10 trimethyltridecane; NPr: Norpristane; Pr: Pristane; Ph: Phytane; MMA: Mid-chain methyl-branched alkanes; G: Gammacerane; MG: Methylgammacerane (likely 2-methylgammacerane). Diagonal crosses: Siloxanes (GC column or septum bleeding). The chromatograms are scaled to the most abundant peak in each trace

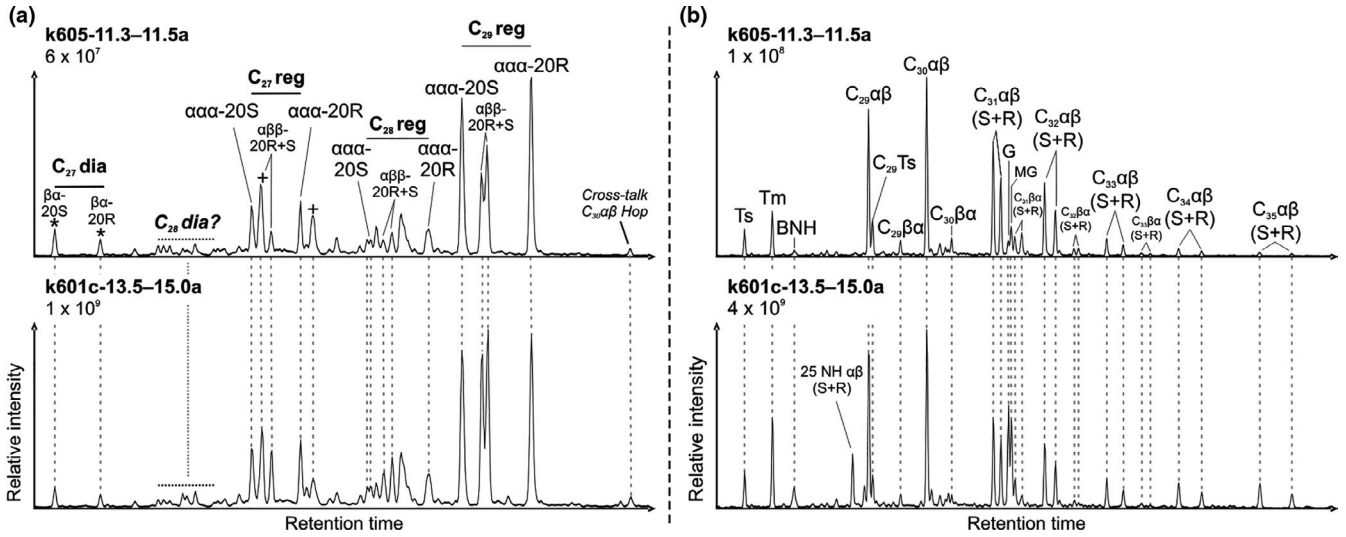

FIGURE 5 MRM–GC–MS ion chromatograms of saturated hydrocarbon fractions. (a) Summed sterane channels (*m/z* 217). Note the different abundances of αββ R + S relative to ααα S + R isomers, here probably indicating fluctuating aquatic salinities. Asterisk: C_{27} diasteranes (βα 20S + R); Cross = C_{29} diasteranes (βα 20S + R). Note that the C_{29} diasterane βα 20S isomer coelutes with the C_{27} regular sterane αββ R isomer. (b) Summed hopane channels (*m/z* 191). Note the presence of gammacerane (G) and a methylgammacerane (likely 2-methylgammacerane; MG). Relative abundances of G and C_{35} homohopanes vary significantly between different samples, suggesting changes in stratification, salinity, and oxygenation of the environment. The chromatograms are scaled to the most abundant peak in each trace

In addition to alkanes, all samples contain abundant acyclic isoprenoids. These include 2,6,10-trimethyldodecane (farnesane, Farn), 2,6,10-trimethyltridecane (TMTD), 2,6,10-trimethylpentadecane (norpristane, NPr), 2,6,10,14-tetramethylpentadecane (pristane, Pr), and 2,6,10,14-tetramethylhexadecane (phytane, Ph) (Figure 4).

4.3.2 | Steranes

All analyzed samples contain cholestane (C_{27}), ergostane (C_{28}), and stigmastane (C_{29}) isomers (5α(H),14α(H),17α(H) 20S + 20R and 5α(H),14β(H),17β(H) 20R + 20S) (Figure 5a). The C_{29} steranes represent the most prominent pseudohomologues (62–73% relative to total C_{27}–C_{29} steranes; Table 2). C_{30} steranes such as 24-isopropylcholestane (24-ipc) and 26-methylstigmastane (26-mes) are only present in minor traces and difficult to quantify accurately (Figure 6).

Some samples also comprise traces of ring methylated and dimethylated varieties of stigmastane (i.e., 30 and 31 carbon atoms, respectively). Furthermore, all samples contain a suite of short-chain steranes (typically C_{21}-C_{24}), including 5α(H),14β(H),17β(H)-pregnane and 20-methyl-5α(H),14β(H),17β(H)-pregnane (diginane and 20-methyldiginane, respectively, see Requejo, Hieshima, Hsu, McDonald, & Sassen, 1997; Wingert & Pomerantz, 1986). Diasteranes are also present in all samples but consistently less abundant than the corresponding regular steranes (Figure 5a).

4.3.3 | Hopanes and tricyclic terpanes

All samples contain C_{30} hopanes (αβ and βα; possibly C_{30} Ts, see Farrimond & Telnæs, 1996) and the C_{31}–C_{35} homohopane isomers (17α(H),21β(H) 22S + 22R and 17β(H),21α(H) 22S + 22R) (Figure 5b). Further compounds are 22,29,30-trisnorhopanes (C_{27} Ts and Tm), bisnorhopane (C_{28}; likely 29,30 rather than 28,30 because *m/z* 355 is virtually absent in the mass spectra, see Summons & Powell, 1987) and 30-norhopanes (C_{29} 17α(H),21β(H) and 17β(H),21α(H); C_{29} Ts). Some samples contain traces of 25-bisnorhopane (C_{28}; likely 25,28 because *m/z* 341 is absent in the mass spectra, see Aguiar, Júnior, Azevedo, & Neto, 2010) and 25-norhopanes (C_{29} 17α(H),21β(H) and 17β(H),21α(H)) (Figure 5b). Sample k601c-13.5–15.0a additionally comprises traces of methylhopanes.

All samples contain minor amounts of short-chain tricyclic terpanes ≤C_{25} and 17,21-secohopanes (particularly the C_{24} variety, as confirmed by MRM–GC–MS analyzes).

4.3.4 | Gammacerane and methylgammacerane

Gammacerane abundances show significant variations in different facies (GI = 0.6–5.7), but also within a distinct black shale to marl horizon (GI = 5.7 and 2.3 in samples k601c-13.5–15.0a and k601c-13.5–15.0b, respectively) (Figure 5b, Table 2). Some samples additionally contain a putative methylgammacerane (likely 2-methylgammacerane; Figures 5b and 7). Relative abundances of this compound appear to be decoupled from those of

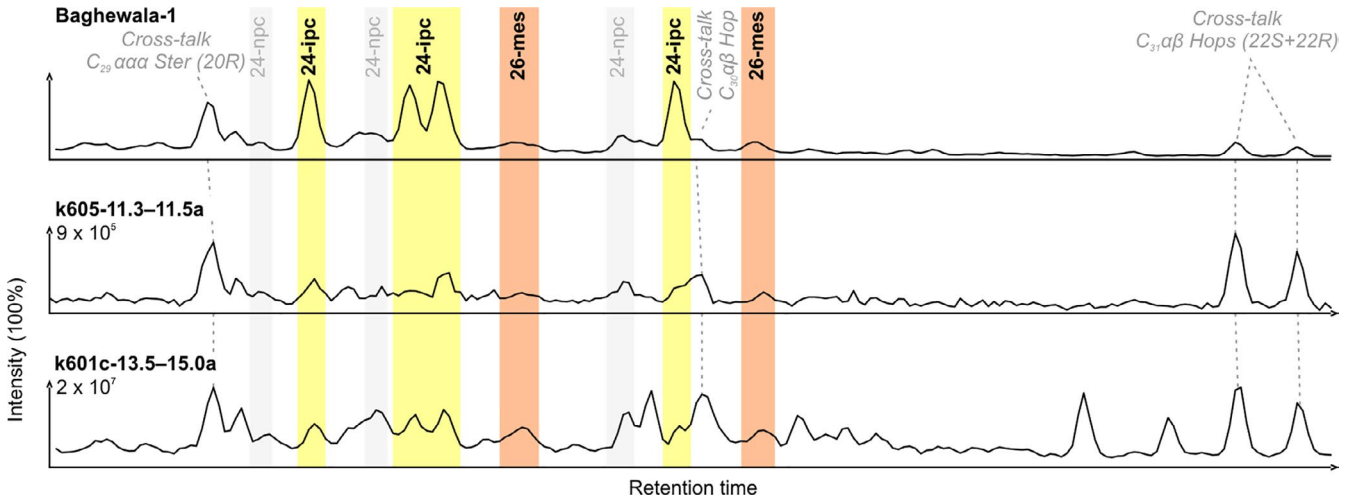

FIGURE 6 MRM–GC–MS ion chromatograms of C_{30} sterane distributions (414 → 217 Da ion transitions) in selected Khatyspyt samples. The C_{30} sterane trace for an Ediacaran–Cambrian reference sample (Baghewala-1 oil, India; Peters, Clark, Gupta, McCaffrey, & Lee, 1995) containing 26-methylstigmastane (26-mes, orange), 24-isopropylcholestane (24-ipc, yellow), and 24-*n*-propylcholestane (24-npc, gray) is provided for comparison. Note that 24-ipc and 26-mes are ≤0.4% and ≤0.2% of the total C_{27}–C_{30} regular steranes, respectively, and that these values are probably even overestimated due to low signal-to-noise ratios and cross talk effects. The chromatograms are scaled to the most abundant peak in each trace

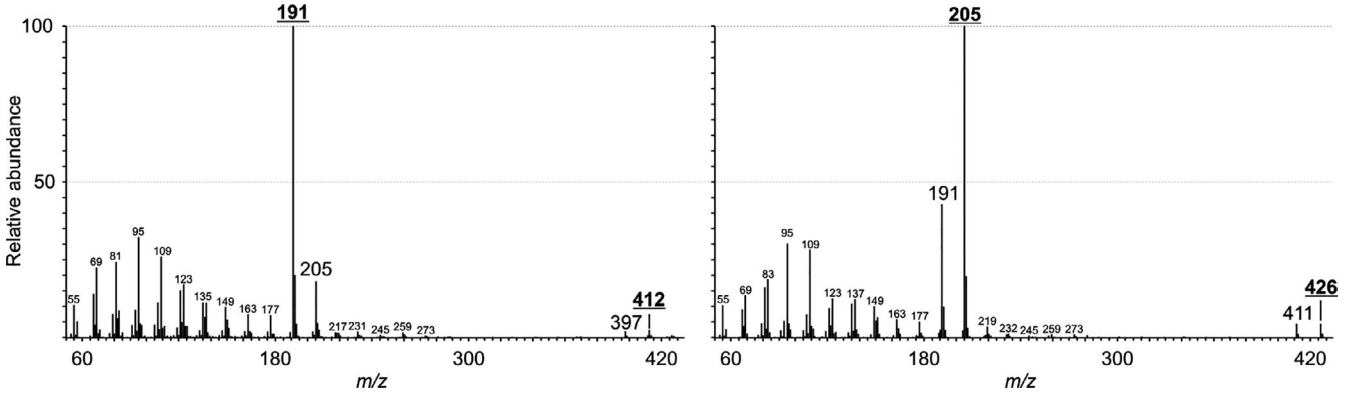

FIGURE 7 Background-subtracted mass spectra of gammacerane (left) and the putative 2-methylgammacerane (right). The methylgammacerane has a characteristic main fragment ion of *m/z* 205 instead of 191 due to the presence of an additional methyl group (likely at position C-2). Note the absence of fragment ions at *m/z* 369 or 383 which are characteristics of the hopane and methylhopane series, respectively

gammacerane (MGI = 1.7–5.6). Within the distinct black shale to marl horizon, however, relative methylgammacerane and gammacerane abundances change similarly (MGI = 3.6 and 1.7 in samples k601c-13.5–15.0a and k601c-13.5–15.0b, respectively) (Figure 5b, Table 2).

4.3.5 | Further cyclic aliphatic hydrocarbons

All samples contain low abundances of C_{15}–C_{20} bicyclic sesquiterpanes. Two of the analyzed samples (k601c-13.5–15.0a, k601c-6.0) contain minor traces of β-carotane.

5 | DISCUSSION

5.1 | Geobiology of the Khatyspyt Lagerstätte—inferences from sedimentary facies

The alternating micritic to fine-grained layers (Figure 2a) represent allochthonous event deposits (Table 2). Organic laminae that interweave sedimentary grains (Figure 2b,f), in contrast, are remnants of microbial mats that thrived in the Khatyspyt environment (Table 2). It should be noted, however, that these microbial laminae are easily confused with diagenetic pressure solution seams that can be identified by irregular and sutured grain contacts. All these features are remarkably similar to the Shibantan Member in South China and emphasize the intimate relationship between allochthonous event deposits and microbial mat growth (compare Duda, 2014; Duda, Blumenberg, et al., 2014; Duda et al., 2015). As in case of the Shibantan Member, the continuous delivery of allochthonous material from adjacent ramp environments likely stimulated microbial mat growth by providing fertile substrates. Bituminous limestones that are not laminated on the microfacies scale (Figure 2e) are either part of a thick allochthonous event deposit or represent an in situ formed carbonate sludge (Table 2).

Sparry calcite overgrowth cements in grainy layers (Figure 2f) are an important trait of the Khatyspyt Formation. Similar cements are also widespread in limestones of the Shibantan Member in South China (own observations). At both locations, sparry calcite overgrowth cements are restricted to coarse-grained layers, indicating that porosity is an important prerequisite for their formation. Notably, layers exhibiting sparry calcite overgrowth cements typically occur underneath very fine-grained allochthonous material or microbial mats (Figure 2f). It is therefore tempting to speculate that sedimentary sealing as well as microbial activity factored into the formation of the sparry calcite overgrowth cements.

The observed circular to oval structures filled with cements or grains (Figure 3a,b) are classic traces of burrowing organisms. Similar trace fossils are also known from the Shibantan Member (Xiao, Chen, Zhou, & Yuan, 2019; own observations). In both settings, these traces are horizontal and spatially associated with microbial mats (Table 2). Such traces were likely produced by burrowers that exploited microbial mats for resources such as food and oxygen (Gehling, 1999; Gingras et al., 2011; Seilacher & Pflüger, 1994).

Vertically extending structures exhibiting fishhook- and antler-like shapes in cross section (Figure 3b,c) are typically produced by organisms that exploit deeper sediment levels (Table 2). These structures possibly represent sections of individual *Nenoxites* menisci. Likewise, disturbed bedding associated with mottled fabrics and structures (Figures 2d and 3d) is a characteristic feature of ichnofabrics produced by vertical burrowers. This interpretation is also in good accordance with the associated sparitic structures (Figure 2d), as burrows are commonly sites of selective replacement and preferential cementation. All these structures and fabrics were observed in samples from the upper part of the succession (Figure 1; Table 2) and add to findings of meniscate burrows in the Khatyspyt ecosystem (Rogov et al., 2012, 2015). This highlights the presence of diverse burrowing strategies in the terminal Ediacaran, including vertical exploitation of sediment as known from the Phanerozoic.

5.2 | Biomarker data integrity (thermal maturity, biodegradation & syngeneity)

Rock-Eval pyrolysis is an established tool used to assess the thermal maturity of rocks (e.g., Espitalié et al., 1977; Peters, 1986; Tissot & Welte, 1984). Sample k601c-6.0 exhibits a PI >0.2 which might indicate the presence of migrated oil (see Peters, 1986). On the other hand, the Rock-Eval T_{max} value (437°C) is consistent to the other samples (429–432°C) (Table 3). However, Rock-Eval parameters (T_{max}, HI, OI) and lipid biomarker data cannot be considered absolutely valid for this sample and are therefore excluded.

Reliable Rock-Eval T_{max} values of ≤432°C (Table 3) suggest early oil window maturity levels, significantly prior to peak oil generation (see Peters, 1986). This is generally in accordance with reliable HI and OI values. The remarkable range of these data (HI = 253–419 mg HC/g TOC; OI = 19–105 CO_2/g TOC: Table 3) likely reflects substantial variations in biogenic source inputs and environmental conditions. Taken together, robust and reliable Rock-Eval data demonstrate that the thermal maturity of Khatyspyt organic matter is suitable for detailed lipid biomarker investigations.

Molecular parameters are a further important tool to constrain the thermal maturity of organic matter (Killops & Killops, 2005; Mißbach, Duda, Lünsdorf, Schmidt, & Thiel, 2016; Peters et al., 2005; Tissot & Welte, 1984). Elevated abundances of 17β(H),21α(H)-hopanes (Figure 5b) support the inferred early oil window maturity levels. This assessment is in good accordance with C_{31} hopane isomerization [22S/(S + R) = 0.57–0.60], C_{27} hopane ratios [Ts/(Ts + Tm) = 0.27–0.37], and C_{29} sterane isomerization [20S/(S + R) = 0.47–0.52; ββ/(ββ + αα) = 0.30–0.55) (Mackenzie, Patience, Maxwell, Vandenbroucke, & Durand, 1980; Moldowan et al., 1991; Moldowan, Sundararaman, & Schoell, 1986; Seifert & Moldowan, 1978, 1980, 1986) (Table 1). Low MPR, MPI-1, and R_c values (≤1.45, ≤0.65, and ≤0.68, respectively) are also consistent with an early oil-generative stage (Boreham et al., 1988; Killops & Killops, 2005; Radke & Welte, 1983). It should be noted, however, that the MPI-1 was originally developed for terrestrial organic matter (Radke et al., 1982) and that only values of ≥0.7 might be robust to assess the thermal maturity of Proterozoic organic matter (Boreham et al., 1988).

The analyzed samples typically exhibit high abundances of low carbon number *n*-alkanes and no obvious hump due to an appreciable UCM (Figure 4), indicating that alteration by secondary processes such as biodegradation or weathering is minor (e.g., Peters et al., 2005; Tissot & Welte, 1984). However, the presence of 25-norhopanes in some of the samples potentially indicates slight biodegradation during early diagenesis, burial, or later exposure (Bennett, Fustic, Farrimond, Huang, & Larter, 2006; Blanc & Connan, 1992; Moldowan & McCaffrey, 1995; Peters, Moldowan, McCaffrey, & Fago, 1996; Seifert & Moldowan, 1979). Indeed, these compounds appear to be particularly abundant in samples that virtually exhibit low *n*-alkane to sterane and hopane ratios (k601c-13.5–15.0a: Figures 4 and 5b). However, the restriction of 25-norhopanes to a few varieties and the absence of complete suite of homologs points against severe biodegradation (Moldowan & McCaffrey, 1995). Thus, the effect of biodegradation appears to be negligible for the analyzed samples.

5.3 | Geobiology of the Khatyspyt Lagerstätte—inferences from the biomarker record

5.3.1 | Biological sources and paleo-community structure

Photoautotrophic cyanobacteria and/or algae were major biological sources of organic matter in the Khatyspyt Lagerstätte as evidenced by abundant chlorophyll-derived acyclic isoprenoids such as pristane and phytane in all samples (e.g., Bendoraitis, Brown, & Hepner, 1962; Peters et al., 2005; Philp, 1985; Tissot & Welte, 1984). Both sources could also account for the observed bicyclic sesquiterpanes (Alexander, Kagi, & Noble, 1983; Alexander, Kagi, Noble, & Volkman, 1984; Pu, Yaorong, & Baisheng, 1991). The presence of bacteria is further evidenced by abundant hopanes and, possibly, cyclohexylalkanes (de Rosa, Gambacorta, Minale, & Bu'Lock, 1971; Ourisson, Albrecht, & Rohmer, 1979; Rohmer, Bouvier-Navé, & Ourisson, 1984; Suzuki, Saito, Kawaguchi, Okuda, & Komagata, 1981). Important groups likely included cyanobacteria (mid-chain branched alkanes: Gelpi, Schneider, Mann, & Oro, 1970; Shiea, Brassell, & Ward, 1990) and sulfate-reducing bacteria (*iso*- and *anteiso*-alkanes, see Kaneda, 1991; pyrite crystals). It should be noted, however, that cyclohexylalkanes and *iso*- and *anteiso*-alkanes might also be of diagenetic or catagenetic origin (Gelin et al., 1994; Kissin, 1987; Rubinstein & Strausz, 1979). Mid-chain methyl-branched alkanes ("*X-peaks*") in the C_{20}–C_{26} range are not particularly abundant and therefore not indicative for a specific biological source.

The vast majority of regular steranes in the rock record derive from eukaryotes (Summons, Bradley, Jahnke, & Waldbauer, 2006; Volkman, 1986, 2003; Wei, Yin, & Welander, 2016). The consistent dominance of stigmastane (C_{29}) over other sterane homologues in the Khatyspyt Formation (62–73% relative to total C_{27}–C_{29} steranes; Table 2) is typical for Ediacaran rocks and oils and commonly explained by abundant chlorophytes as primary producers (see Grantham, 1986; Knoll, Summons, Waldbauer, & Zumberge, 2007; Kodner, Pearson, Summons, & Knoll, 2008; Summons & Walter, 1990). Mega-algae might be an additional source for stigmastane in the Khatyspyt Lagerstätte, but the relative importance of these organisms in terms of total biomass remains unknown. Notably, the Khatyspyt record spans between relative stigmastane abundances reported for the Ediacaran of central and southwestern Baltica (55%–60%: Goryl, Marynowski, Brocks, Bobrovskiy, & Derkowski, 2018; 59% in average: Pehr et al., 2018), the Neoproterozoic–Cambrian of South Oman (70% in average: Grosjean, Love, Stalvies, Fike, & Summons, 2009), and the Ediacaran of northeastern Baltica (i.e., the Russian White Sea; 75% in average: Bobrovskiy, Hope, Golubkova, & Brocks, 2020).

Sterane/hopane ratios are consistently low in the Khatyspyt Lagerstätte (0.07–0.30 in the samples analyzed herein; Table 2; 0.37

in Duda et al., 2016, not included in this sample set), thus suggesting higher relative inputs by bacteria as compared to eukaryotes. A preferential breakdown of steranes through thermal stress can be excluded as all analyzed samples are in a maturity range in which these compounds remain stable (see, e.g., Mißbach et al., 2016). A taphonomic suppression of steranes through microbial mats ("mat seal effect": Pawlowska, Butterfield, & Brocks, 2013; Blumenberg, Thiel, & Reitner, 2015; Shen, Thiel, Duda, & Reitner, 2018; Lee, Love, Jahnke, Kubo, & Des Marais, 2019) can also be ruled out since the analyzed Khatyspyt facies is demonstrably variable and microbial mats appear to be absent in some cases (Figure 2; Table 2). Therefore, the observed scarcity of steranes most likely reflects a primary ecological fingerprint.

The ratio of eukaryotic steranes to bacterial hopanes is a well-established measure for the relative importance of the two domains in ancient settings (e.g., Peters et al., 2005). Sterane/hopane ratios <1 (or hopane/sterane ratios >1) reflect higher relative inputs by bacteria as compared to eukaryotes. The sterane/hopane ratios observed in the Khatyspyt Formation are systematically lower than those from Neoproterozoic–Lower Cambrian records of eastern Siberia (0.47–4.63, mean 1.18: Kelly, Love, Zumberge, & Summons, 2011) and South Oman (ca. 0.40–1.30, mean 0.83: Grosjean et al., 2009; Love et al., 2009). At the same time, they are well in line with Ediacaran records of central and southwestern Baltica, where sterane/hopane ratios range between 0.01 and 0.63 (mean = 0.05) and sterane/(C_{30} + C_{31} hopane) ratios range between 0.02 and 0.47 (mean = 0.20) (Pehr et al., 2018 and Goryl et al., 2018, respectively). They are also in good accordance with reported values from northeastern Baltica (i.e., the Russian White Sea; 0.06–0.59, mean = 0.20), particularly in case of intervals with Ediacara-type fossils (0.06–0.43, mean = 0.20) (Bobrovskiy et al., 2020, their supplementary Table 1).

Taken together, sterane/hopane ratios from all records with assemblages of Ediacara-type fossils are all well below 1, reflecting higher relative inputs by bacteria as compared to eukaryotes. This suggests that not all communities with Ediacara-type organisms inhabited algal-rich environments, as proposed elsewhere (Bobrovskiy et al., 2020). Furthermore, only the highest of these values fall into the lowermost average range of post-Ediacaran rocks and oils (i.e., 0.5–2.0, mean = 1.0: Cao et al., 2009; Peters et al., 2005), calling the proposed similarity to nutrient-replete Phanerozoic ecosystems (Bobrovskiy et al., 2020) into question. All lipid biomarker data available for successions with Ediacara-type fossils suggest rather oligotrophic environments dominated by bacteria. It remains to be tested whether these baseline conditions also prevailed elsewhere in other ecosystems with Ediacara-type organisms.

5.3.2 | Evidence for the presence of early animals?

C_{30} regular steranes with unusually alkylated side chains (i.e., 24-ipc and 26-mes) have been utilized as lipid biomarkers to track early animals (Love et al., 2009; McCaffrey et al., 1994; Zumberge, 2019; Zumberge, Cárdenas, Duda, Sperling, & Love, 2019; Zumberge et al., 2018). This is because demosponges are the only extant organisms known to biosynthesize 24-ipc and 26-mes precursors as major lipids, ranging up to 99 wt.% of their total sterols (e.g., Djerassi & Silva, 1991; Giner, 1993; Hofheinz & Oesterhelt, 1979; Zumberge, 2019; Zumberge et al., 2018). Reported traces of possible 24-ipc and 26-mes precursors in modern rhizarian protists (down to <0.01% of total steroids; Nettersheim et al., 2019), in contrast, appear to be problematic and are subject of an ongoing discussion (Hallmann et al., 2020; Love et al., 2020).

In the samples analyzed herein, 24-ipc and 26-mes are only present in minor traces (≤0.4% and ≤0.2% of the total C_{27}–C_{30} regular steranes, respectively) (Figure 6). The calculated relative abundances are probably even overestimated due to low signal-to-noise ratios and cross talk effects. Given the low thermal maturity of organic matter in the Khatyspyt Formation (Duda et al., 2016; results of this study), a preferential loss due to thermal stress ("*thermal taphonomy*": Mißbach et al., 2016) appears unlikely. At the same time, low quantities of these compounds might form through diagenetic side chain modification of C_{29} sterols, although this requires further investigation. In any case, organisms capable of directly synthesizing 24-ipc and 26-mes were not widespread in the Khatyspyt Lagerstätte.

Late Ediacaran strata from Baltica contain similarly low amounts of these source-specific biomarkers, with 24-ipc being ≤0.6% relative to the total C_{27}–C_{30} sterane ratios and below detection limits in over half the sample set (Pehr et al., 2018). This is at least an order of magnitude lower than in Neoproterozoic rocks and oils from other localities such as South Oman, where 24-ipc and 26-mes typically account for 1%–4% of the total C_{27}–C_{30} steranes (Grosjean et al., 2009; Love et al., 2009; McCaffrey et al., 1994; Zumberge, 2019; Zumberge et al., 2018, 2019). This suggests that Ediacara-type organisms and mega-algae occupied different niches than demosponges (oligotrophic vs eutrophic, respectively).

5.3.3 | Methylgammacerane

Some of the analyzed samples contain a putative methylgammacerane (likely 2-methylgammacerane) (Figures 5b and 7). High amounts of 2-methylgammacerane have previously been reported from Cambrian "*Q Oils*" in North Oman (Grosjean, Love, Kelly, Taylor, & Summons, 2012). 2-methylgammacerane (C_{31}) coelutes with/near 3β-methylhopanes, C_{31}βα homohopanes (S + R), and gammacerane (C_{30}) (Grosjean et al., 2012). Peaks of these compounds are commonly not fully separated and switch their elution order depending on chromatographic conditions. As a consequence, methylgammacerane may elute slightly prior to gammacerane, despite having a higher molecular weight (M^+ of 426 vs M^+ of 412). This chromatographic behavior is also known from tetrahymanol and 2-methyltetrahymanol acetates (see Rashby, Sessions, Summons, & Newman, 2007; Welander, Coleman, Sessions, Summons, & Newman, 2010). However, methylgammacerane can clearly be distinguished from 3β-methylhopanes, C_{31}βα homohopanes (S + R), and gammacerane based on distinct mass spectral characteristics (i.e., main fragment

ion at *m/z* 205, absence of fragment ions at *m/z* 369 or 383, and a molecular ion at *m/z* 426: Figure 7). For the samples analyzed herein, this interpretation was further corroborated by MRM–GC–MS (Figure S3).

Tetrahymanol is an abundant lipid in bacterivorous ciliates (Harvey & McManus, 1991; ten Haven, Rohmer, Rullköter, & Bisseret, 1989; Sinninghe Damsté et al., 1995) and anoxygenic phototrophs (*Rhodopseudomonas palustris*; Kleemann et al., 1990; Eickhoff, Birgel, Talbot, Peckmann, & Kappler, 2013). Methyltetrahymanols (particularly 2-methyltetrahymanol) have been reported in cultures of *Bradyrhizobium japonicum* and *R. palustris* (Bravo, Perzl, Härtner, Kannenberg, & Rohmer, 2001; Eickhoff et al., 2013; Rashby et al., 2007; Welander et al., 2009). It has been suspected that 2-methyltetrahymanol is a useful marker for anoxygenic phototrophic bacteria (Eickhoff et al., 2013). Indeed, layers of modern microbial mats that are inhabited by anoxygenic phototrophs were found to be enriched with 2-methyltetrahymenols, suggesting purple sulfur bacteria as a source (Lee, 2016). The occurrence of methylated tetrahymanols in extant organisms strongly suggests a primary origin of methylgammacerane in ancient sedimentary rocks. The decoupled gammacerane and methylgammacerane abundances (MGI = 1.7–5.6: Table 2) potentially indicate different biological sources for both compounds.

By analogy to A-ring methylated steranes, diagenetic alkylation of tetrahymanol may constitute an alternative source for the observed methylgammacerane. A-ring methylated steroids form via alkylation of Δ^2-sterene intermediates—therefore resulting in 2- and 3-alkylsteranes (see Summons & Capon, 1988, 1991). Alternatively, a diagenetic alkylation of the hydroxyl group in tetrahymanol (i.e., C-3) appears conceivable. Knowledge on the exact alkylation site(s) could thus help to assess a potential diagenetic origin of methylgammacerane in the Khatyspyt Lagerstätte. Unfortunately, it is unclear whether isomers methylated at different carbon positions can be distinguished under the chromatographic conditions used herein. However, methylgammacerane in Oman is suspected to be mainly alkylated at C-2 (Grosjean et al., 2012), and potential precursors are well known from extant organisms—in contrast to 2- and 3-methylsteranes (Brocks & Summons, 2003). Furthermore, methylgammacerane abundances seem to be decoupled from gammacerane (see above). Therefore, a biological origin of methylgammacerane appears likely, although a diagenetic origin cannot completely be excluded.

5.3.4 | Paleoenvironmental conditions

CPI values of ~1 and the predominance of short-chain *n*-alkanes with maxima at ≤*n*-C_{19} indicate a marine environment (Peters et al., 2005) (Figure 4, Table 1). This is in good accordance with Ediacaran records from South China (Duda, Blumenberg, et al., 2014; Duda et al., 2015) and the Russian White Sea (Grazhdankin, 2003). Neoproterozoic–Cambrian sedimentary rocks in Oman were also mostly deposited in marine environments (Gorin, Racz, & Walter, 1982), while parts of Baltica were possibly temporarily affected by freshwater conditions (Bojanowski et al., 2020).

Differences in the TOC contents (0.12–2.22 wt.%: Table 3) and biomarker assemblages suggest changing environmental conditions in the Khatyspyt Lagerstätte. For instance, strikingly varying abundances of gammacerane in the analyzed samples (GI = 0.8–5.7: Table 2) and in previous studies (no gammacerane: Duda et al., 2016) indicate changes in water column stratification and, possibly, salinity (see Moldowan, Seifert, & Gallegos, 1985; ten Haven et al., 1989; Sinninghe Damsté et al., 1995; ten Haven, de Leeuw, & Schenck, 1985; ten Haven et al., 1988; Figure 5b; Table 2). Changes in the relative abundance of C_{35} homohopanes (C_{35} homohopane index = 0.1–0.2) and regular αββ sterane isomers (αββ R + S vs ααα S + R dominances) also indicate fluctuations in salinity and oxygenation (see Farrimond et al., 2003; ten Haven, de Leeuw, Peakman, & Maxwell, 1986; Peakman, ten Haven, Rechka, de Leeuw, & Maxwell, 1989; Peters & Moldowan, 1991; Summons & Powell, 1992; ten Haven et al., 1988; Bishop & Farrimond, 1995; Figure 5; Table 2). In concert, these data suggest that organisms in the Khatyspyt Lagerstätte were confronted with dynamically changing environmental conditions. This is in good accordance with findings from the Shibantan Member (Duda, 2014; Duda, Blumenberg, et al., 2014; Duda et al., 2015; Xiao et al., 2020).

5.4 | Geobiology of the Khatyspyt Lagerstätte—a synthesis

The Khatyspyt Formation was deposited in marine carbonate ramp environments, very similar to the contemporaneous Shibantan Member in South China (see Duda, 2014; Duda, Blumenberg, et al., 2014; Duda et al., 2015). Such environments react sensitively on abiotic and biological influences. It is therefore not surprising that organisms in both systems were confronted with frequently changing chemical conditions and nutrient availabilities. The resulting fluctuating selection pressures likely promoted the development of pioneering physiological strategies and innovative lifestyles in different organism groups. It is tempting to speculate that these innovations eventually provided evolutionary advantages in times of global environmental change.

Occurrences of macroscopic complex fossils appear to be linked to specific ecological conditions. For instance, the most diverse assemblages of Ediacara-type fossils occur in facies characterized by prominent microbial mats and horizontal traces (k601c-13.5–15.0a, b; Figures 2b and 3a). Lipid biomarkers indicate a stratified marine environment, normal to moderately elevated salinities, and low oxygen levels (GI = 2.3–5.7; C_{35} homohopane index = 0.1–0.2; equally important αββ R + S and ααα S + R sterane isomers: Figure 5, Table 2). Such conditions are widely considered problematic for macroscopic complex organisms. However, certain Avalon-type macro-organisms (rangeomorphs, arboreomorphs) may develop tolerances and/or life strategies that allowed them to cope with these ecological stressors (e.g., symbiotic lifestyles,

interaction with microbial mat communities; see also Bykova et al., 2017).

Mega-algae, in contrast, are most abundant and diverse in facies that lack evidence for the presence of prominent microbial mats but are dominated by layers that represent allochthonous event deposits (samples k605-11.3–11.5a, b: Figure 2a). Lipid biomarkers in these samples indicate a non-stratified marine environment and normal salinities during deposition (GI = 0.6–0.8; C_{35} homohopane index = 0.1; dominant ααα S + R sterane isomers: Figure 5, Table 2; see also Duda et al., 2016). In contrast to the environments described above, such conditions appear to be favorable for macroscopic complex organisms. It seems conceivable that mega-algae proliferated in times of intermittent event deposition, but this remains to be further tested in futures studies.

The Khatyspyt Lagerstätte shares some striking similarities with the Shibantan Member, including sedimentary facies and occurrences of Ediacara-type fossils. Unfortunately, however, lipid biomarkers are not well preserved in the Shibantan Member (Duda, Blumenberg, et al., 2014; Duda, Thiel, et al., 2014). A variety of lipid biomarker characteristics of the Khatyspyt Lagerstätte are similar to the Baltica record (e.g., low sterane/hopane ratios, scarcity of C_{30} steranes; Goryl et al., 2018, Pehr et al., 2018). These lipid biomarker records, as well as reported low sterane/hopane ratios from the Russian White Sea (Bobrovskiy et al., 2020), suggest that the ecosystems were oligotrophic and dominated by bacteria. Furthermore, organisms capable of directly synthesizing the C_{30} steranes 24-ipc and 26-mes (most likely candidates demosponges) appear not to have been widespread in these environments (Table 2).

Despite these similarities, the Khatyspyt Lagerstätte is special in that it exhibits assemblages of carbonaceous compression fossils (mega-algae), ichnofabrics produced by vertical burrowers, and very low to high TOC contents (0.12–2.22 wt.%; Table 3). In Baltica, TOC contents are mostly ≤0.5 wt.% and rarely exceed 1.0 wt.% (Goryl et al., 2018; Pehr et al., 2018). In South Oman, in contrast, TOC contents are mostly >1.0 wt.% and range up to 11.0 wt.% (Grosjean et al., 2009; Love et al., 2009). The Khatyspyt record thus ecologically bridges between Baltica and South Oman. At the same time, the unique features of the Khatyspyt Lagerstätte demonstrate that Ediacaran ecosystems were more highly diverse than previously realized. Furthermore, it emphasizes the impact of sedimentary processes and various environmental controls (water column stratification, oxygen, and possibly salinity levels) on the distribution of Avalon-type macro-organisms and mega-algae (Table 2).

6 | CONCLUSIONS

Bituminous facies of the Khatyspyt Formation were deposited in marine carbonate ramp environments. Consistently low sterane/hopane ratios reflect relatively low inputs of eukaryotic organisms to the preserved organic matter, suggesting oligotrophic marine depositional environments in which bacteria were dominant. This is similar to lipid biomarker findings from other successions with Ediacara-type fossils (Baltica, including the Russian White Sea). C_{30} steranes such as 24-isopropylcholestane and 26-methylstigmastane are present in minor traces but do not appear to be completely absent. Thus, Avalon-type organisms occupied different niches than organisms capable of directly synthesizing C_{30} sterane precursors among their major lipids. Notably, some of the analyzed samples contain a putative methylgammacerane (possibly 2-methylgammacerane), which was likely sourced by organisms (ciliates, anoxygenic phototrophs, and/or purple sulfur bacteria) and may be a good proxy for stratification. Striking variation in the relative abundances of C_{35} homohopanes, gammacerane, and methylgammacerane likely reflects overall community structures and environmental fluctuations in the Khatyspyt Lagerstätte. The most diverse assemblages of well-preserved rangeomorph and arboreomorph organisms occur in facies characterized by prominent microbial mats and horizontal traces. Lipid biomarkers indicate a stratified marine environment, normal to moderately elevated salinities, and low oxygen levels. Mega-algae, in contrast, are most abundant and diverse in facies that lack evidence for the presence of prominent microbial mats but are dominated by allochthonous event deposits. Lipid biomarkers in these samples indicate a non-stratified marine environment and normal salinities during deposition. Vertical burrowers occur in similar facies but with biomarker evidence for stratification in the water column or around the seafloor. Thus, the distribution of Avalon-type macro-organisms, mega-algae, and burrowers was controlled by sedimentary processes and various environmental factors. It appears plausible that innovative adaptations needed to survive in these habitats eventually provided evolutionary advantages in times of global environmental change. In this view, dynamic settings like the Khatyspyt Lagerstätte could have provided metabolic challenges for sustenance and growth which primed eukaryotic organisms to cope with changing environmental habitats, allowing for a later diversification and expansion of complex macroscopic life in the marine realm.

ACKNOWLEDGMENTS

JPD gratefully acknowledges financial support by the German Research Foundation (DFG; research fellowship DU 1450/4-1, project DU 1450/5-1) and the Research Department of the University of Göttingen. Fieldwork was supported by the Russian Foundation for Basic Research (grant 18-05-70110). VIG, DSM, and DVG are supported by the Russian Science Foundation (grant 20-67-46028). We thank A. Hackmann, A. G. Kral, A. Reimer, B. Röring, B. B. Kochnev, G. Scheeder, H. Mißbach, K. E. Nagovitsin, M. Reinhardt, N. V. Bykova, V. V. Marusin, and W. Dröse for technical and logistic support. This work has greatly benefited from discussions with A. J. Zumberge, I. Bobrovskiy, J. J. Brocks, J. Reitner, T. M. Parfenova, and V. Thiel. We also thank three anonymous reviewers and the editors for thoughtful and constructive comments which helped to improve the manuscript. Research at the Trofimuk Institute of Petroleum Geology and Geophysics has been conducted under Government Contracts 0331-2019-0002 (Ministry of Education and Science of the Russian Federation). Open access funding enabled and organized by Projekt DEAL.

ORCID

Jan-Peter Duda https://orcid.org/0000-0002-8959-097X

REFERENCES

Aguiar, A., Silva Júnior, A. I., Azevedo, D. A., & Aquino Neto, F. R. (2010). Application of comprehensive two-dimensional gas chromatography coupled to time-of-flight mass spectrometry to biomarker characterization in Brazilian oils. *Fuel*, *89*(10), 2760–2768. https://doi.org/10.1016/j.fuel.2010.05.022

Ahmed, M., & George, S. C. (2004). Changes in the molecular composition of crude oils during their preparation for GC and GC–MS analyses. *Organic Geochemistry*, *35*(2), 137–155. https://doi.org/10.1016/j.orggeochem.2003.10.002

Alexander, R., Kagi, R., & Noble, R. (1983). Identification of the bicyclic sesquiterpenes drimane and eudesmane in petroleum. *Journal of the Chemical Society, Chemical Communications*, *5*, 226–228. https://doi.org/10.1039/c39830000226

Alexander, R., Kagi, R. I., Noble, R., & Volkman, J. K. (1984). Identification of some bicyclic alkanes in petroleum. *Organic Geochemistry*, *6*, 63–72. https://doi.org/10.1016/0146-6380(84)90027-5

Bendoraitis, J. G., Brown, B. L., & Hepner, L. S. (1962). Isoprenoid hydrocarbons in petroleum. Isolation of 2,6,10,14-tetramethylpentadecane by high temperature gas-liquid chromatography. *Analytical Chemistry*, *34*(1), 49–53. https://doi.org/10.1021/ac60181a011

Bennett, B., Fustic, M., Farrimond, P., Huang, H., & Larter, S. R. (2006). 25-Norhopanes: Formation during biodegradation of petroleum in the subsurface. *Organic Geochemistry*, *37*(7), 787–797. https://doi.org/10.1016/j.orggeochem.2006.03.003

Bishop, A. N., & Farrimond, P. (1995). A new method of comparing extended hopane distributions. *Organic Geochemistry*, *23*(10), 987–990. https://doi.org/10.1016/0146-6380(95)00074-7

Blanc, P., & Connan, J. (1992). Origin and occurrence of 25-norhopanes: A statistical study. *Organic Geochemistry*, *18*(6), 813–828. https://doi.org/10.1016/0146-6380(92)90050-8

Blumenberg, M., Thiel, V., & Reitner, J. (2015). Organic matter preservation in the carbonate matrix of a recent microbial mat – Is there a 'mat seal effect'? *Organic Geochemistry*, *87*, 25–34. https://doi.org/10.1016/j.orggeochem.2015.07.005

Bobrovskiy, I., Hope, J. M., Golubkova, E., & Brocks, J. J. (2020). Food sources for the Ediacara biota communities. *Nature Communications*, *11*(1), 1–6. https://doi.org/10.1038/s41467-020-15063-9

Bojanowski, M. J., Goryl, M., Kremer, B., Marciniak-Maliszewska, B., Marynowski, L., & Środoń, J. (2020). Pedogenic siderites fossilizing Ediacaran soil microorganisms on the Baltica paleocontinent. *Geology*, *48*(1), 62–66. https://doi.org/10.1130/G46746.1

Boreham, C. J., Crick, I. H., & Powell, T. G. (1988). Alternative calibration of the Methylphenanthrene Index against vitrinite reflectance: Application to maturity measurements on oils and sediments. *Organic Geochemistry*, *12*(3), 289–294. https://doi.org/10.1016/0146-6380(88)90266-5

Bowring, S. A., Grotzinger, J. P., Isachsen, C. E., Knoll, A. H., Pelechaty, S. M., & Kolosov, P. (1993). Calibrating rates of early Cambrian evolution. *Science*, *261*(5126), 1293–1298. https://doi.org/10.1126/science.11539488

Brasier, M., Cowie, J., & Taylor, M. (1994). Decision on the Precambrian-Cambrian boundary stratotype. *Episodes Journal of International Geoscience*, *17*(1), 3–8.

Bravo, J. M., Perzl, M., Härtner, T., Kannenberg, E. L., & Rohmer, M. (2001). Novel methylated triterpenoids of the gammacerane series from the nitrogen-fixing bacterium *Bradyrhizobium japonicum* USDA 110. *European Journal of Biochemistry*, *268*(5), 1323–1331. https://doi.org/10.1046/j.1432-1327.2001.01998.x

Bray, E. E., & Evans, E. D. (1961). Distribution of *n*-paraffins as a clue to recognition of source beds. *Geochimica et Cosmochimica Acta*, *22*(1), 2–15. https://doi.org/10.1016/0016-7037(61)90069-2

Brocks, J. J., & Summons, R. E. (2003). 8.03 - Sedimentary Hydrocarbons, Biomarkers for Early Life. In H. D. Holland, & K. K. Turekian (Eds.), *Treatise on Geochemistry*, *8*, 63–115). Amsterdam: Elsevier-Pergamon.https://doi.org/10.1016/B0-08-043751-6/08127-5

Bykova, N., Gill, B. C., Grazhdankin, D., Rogov, V., & Xiao, S. (2017). A geochemical study of the Ediacaran discoidal fossil *Aspidella* preserved in limestones: Implications for its taphonomy and paleoecology. *Geobiology*, *15*(4), 572–587. https://doi.org/10.1111/gbi.12240

Cao, C., Love, G. D., Hays, L. E., Wang, W., Shen, S., & Summons, R. E. (2009). Biogeochemical evidence for euxinic oceans and ecological disturbance presaging the end-Permian mass extinction event. *Earth and Planetary Science Letters*, *281*(3–4), 188–201. https://doi.org/10.1016/j.epsl.2009.02.012

Cui, H., Grazhdankin, D. V., Xiao, S., Peek, S., Rogov, V. I., Bykova, N. V., … Kaufman, A. J. (2016). Redox-dependent distribution of early macro-organisms: Evidence from the terminal Ediacaran Khatyspyt Formation in Arctic Siberia. *Palaeogeography, Palaeoclimatology, Palaeoecology*, *461*, 122–139. https://doi.org/10.1016/j.palaeo.2016.08.015

Cui, H., Xiao, S., Cai, Y., Peek, S., Plummer, R. E., & Kaufman, A. J. (2019). Sedimentology and chemostratigraphy of the terminal Ediacaran Dengying Formation at the Gaojiashan section, South China. *Geological Magazine*, *156*(11), 1924–1948. https://doi.org/10.1017/S0016756819000293

de Rosa, M., Gambacorta, A., Minale, L., & Bu'Lock, J. D. (1971). Cyclohexane fatty acids from a thermophilic bacterium. *Journal of the Chemical Society D: Chemical Communications*, *21*, 1334a. https://doi.org/10.1039/c2971001334a

Djerassi, C., & Silva, C. J. (1991). Biosynthetic studies of marine lipids. 41. Sponge sterols: Origin and biosynthesis. *Accounts of Chemical Research*, *24*(12), 371–378. https://doi.org/10.1021/ar00012a003

Duda, J.-P. (2014). *Geobiology of bituminous carbonates from the Ediacaran Shibantan Member* (Dengying Formation, South China): Doctoral dissertation, Georg-August-Universität Göttingen. http://hdl.handle.net/11858/00-1735-0000-0023-98F9-3

Duda, J.-P., Blumenberg, M., Thiel, V., Simon, K., Zhu, M., & Reitner, J. (2014). Geobiology of a palaeoecosystem with Ediacara-type fossils: The Shibantan Member (Dengying Formation, South China). *Precambrian Research*, *255*, 48–62. https://doi.org/10.1016/j.precamres.2014.09.012

Duda, J.-P., Rogov, V. I., Melnik, D. S., Love, G. D., Blumenberg, M. M., & Grazhdankin, D. V. (2019). Reading the Siberian Record: Unravelling the Geobiology of the Ediacaran Khatyspyt Lagerstätte (Arctic Siberia, Russia). In *Proceedings*, *29th International Meeting on Organic Geochemistry*. EAGE Publications, BV Netherlands. https://doi.org/10.3997/2214-4609.201903056

Duda, J.-P., Thiel, V., Reitner, J., & Blumenberg, M. (2014). Assessing possibilities and limitations for biomarker analyses on outcrop samples: A case study on carbonates of the Shibantan Member (Ediacaran Period, Dengying Formation, South China). *Acta Geologica Sinica – English Edition*, *88*(6), 1696–1704. https://doi.org/10.1111/1755-6724.12338

Duda, J.-P., Thiel, V., Reitner, J., & Grazhdankin, D. (2016). Opening up a window into ecosystems with Ediacara-type organisms: Preservation of molecular fossils in the Khatyspyt Lagerstätte (Arctic Siberia). *PalZ*, *90*(4), 659–671. https://doi.org/10.1007/s12542-016-0317-5

Duda, J.-P., Zhu, M., & Reitner, J. (2015). Depositional dynamics of a bituminous carbonate facies in a tectonically induced intra-platform basin: The Shibantan Member (Dengying Formation, Ediacaran Period). *Carbonates and Evaporites*, *31*(1), 87–99. https://doi.org/10.1007/s13146-015-0243-8

Eickhoff, M., Birgel, D., Talbot, H. M., Peckmann, J., & Kappler, A. (2013). Oxidation of Fe(II) leads to increased C-2 methylation of

pentacyclic triterpenoids in the anoxygenic phototrophic bacterium *Rhodopseudomonas palustris* strain TIE-1. *Geobiology*, *11*(3), 268–278. https://doi.org/10.1111/gbi.12033

Espitalié, J., Laporte, J. L., Madec, M., Marquis, F., Leplat, P., Paulet, J., & Boutefeu, A. (1977). Méthode rapide de caractérisation des roches mètres, de leur potentiel pétrolier et de leur degré d'évolution. *Revue De L'institut Français Du Pétrole*, *32*(1), 23–42. https://doi.org/10.2516/ogst:1977002

Farrimond, P., Love, G. D., Bishop, A. N., Innes, H. E., Watson, D. F., & Snape, C. E. (2003). Evidence for the rapid incorporation of hopanoids into kerogen. *Geochimica et Cosmochimica Acta*, *67*(7), 1383–1394. https://doi.org/10.1016/S0016-7037(02)01287-5

Farrimond, P., & Telnæs, N. (1996). Three series of rearranged hopanes in Toarcian sediments (northern Italy). *Organic Geochemistry*, *25*(3–4), 165–177. https://doi.org/10.1016/S0146-6380(96)00127-1

Fedonkin, M. A. (1990). Systematic description of Vendian metazoa. In B. S. Sokolov & A. B. Ivanovskij (Eds.), *The Vendian System: Paleontology*, Vol. *1* (pp. 71–120). Berlin: Springer.

Gehling, J. G. (1991). The case for Ediacaran fossil roots to the metazoan tree. In B. P. Radhakrishna (Ed.) *The world of Martin F. Glaessner*, Geol. Soc. India Mem., Vol. *20* (pp. 181–223). Bangalore: Geological Society of India.

Gehling, J. G. (1999). Microbial mats in terminal proterozoic siliciclastics: Ediacaran death masks. *Palaios*, *14*(1), 40–57. https://doi.org/10.2307/3515360

Gelin, F., de Leeuw, J. W., Sinninghe Damsté, J. S., Derenne, S., Largeau, C., & Metzger, P. (1994). The similarity of chemical structures of soluble aliphatic polyaldehyde and insoluble algaenan in the green microalga *Botryococcus braunii* race A as revealed by analytical pyrolysis. *Organic Geochemistry*, *21*(5), 423–435. https://doi.org/10.1016/0146-6380(94)90094-9

Gelpi, E., Schneider, H., Mann, J., & Oró, J. (1970). Hydrocarbons of geochemical significance in microscopic algae. *Phytochemistry*, *9*(3), 603–612. https://doi.org/10.1016/S0031-9422(00)85700-3

Giner, J. L. (1993). Biosynthesis of marine sterol side chains. *Chemical Reviews*, *93*(5), 1735–1752. https://doi.org/10.1021/cr00021a004

Gingras, M., Hagadorn, J. W., Seilacher, A., Lalonde, S. V., Pecoits, E., Petrash, D., & Konhauser, K. O. (2011). Possible evolution of mobile animals in association with microbial mats. *Nature Geoscience*, *4*(6), 372–375. https://doi.org/10.1038/ngeo1142

Glaessner, M. F. (1984). *The dawn of animal life: A biohistorical study*, Cambridge earth science series. Cambridge, UK: Cambridge University Press.

Gorin, G. E., Racz, L. G., & Walter, M. R. (1982). Late Precambrian-Cambrian sediments of Huqf Group, Sultanate of Oman (12th ed.). *AAPG Bulletin*, *66*(12), 2609–2627.

Goryl, M., Marynowski, L., Brocks, J. J., Bobrovskiy, I., & Derkowski, A. (2018). Exceptional preservation of hopanoid and steroid biomarkers in Ediacaran sedimentary rocks of the East European Craton. *Precambrian Research*, *316*, 38–47. https://doi.org/10.1016/j.precamres.2018.07.026

Grantham, P. J. (1986). The occurrence of unusual C_{27} and C_{29} sterane predominances in two types of Oman crude oil. *Organic Geochemistry*, *9*(1), 1–10. https://doi.org/10.1016/0146-6380(86)90077-X

Grazhdankin, D. V. (2003). Structure and depositional environment of the Vendian Complex in the southeastern White Sea area. *Stratigraphy and Geological Correlation*, *11*(4), 313–331. https://doi.org/10.1134/S0869593809050025

Grazhdankin, D. V., Balthasar, U., Nagovitsin, K. E., & Kochnev, B. B. (2008). Carbonate-hosted Avalon-type fossils in arctic Siberia. *Geology*, *36*(10), 803–806. https://doi.org/10.1130/G24946A.1

Grazhdankin, D. V., Marusin, V. V., Izokh, O. P., Karlova, G. A., Kochnev, B. B., Markov, G. E., … Kaufman, A. J. (2020). Quo vadis, Tommotian? *Geological Magazine*, *157*(1), 22–34. https://doi.org/10.1017/S0016756819001286

Grazhdankin, D. V., Nagovitsin, K. E., Golubkova, E., Karlova, G., Kochnev, B. B., Rogov, V., & Marusin, V. (2020). Doushantuo-Pertatataka–type acanthomorphs and Ediacaran ecosystem stability. *Geology*, *48*(7), 708–712. https://doi.org/10.1130/G47467.1

Grosjean, E., Love, G. D., Kelly, A. E., Taylor, P. N., & Summons, R. E. (2012). Geochemical evidence for an Early Cambrian origin of the 'Q' oils and some condensates from north Oman. *Organic Geochemistry*, *45*, 77–90. https://doi.org/10.1016/j.orggeochem.2011.12.006

Grosjean, E., Love, G. D., Stalvies, C., Fike, D. A., & Summons, R. E. (2009). Origin of petroleum in the Neoproterozoic-Cambrian South Oman Salt Basin. *Organic Geochemistry*, *40*(1), 87–110. https://doi.org/10.1016/j.orggeochem.2008.09.011

Hallmann, C., Nettersheim, B. J., Brocks, J. J., Schwelm, A., Hope, J. M., Not, F. … Stuhr, M. (2020). Reply to: Sources of C_{30} steroid biomarkers in Neoproterozoic-Cambrian rocks and oils. *Nature Ecology and Evolution*, *4*, 37–39. https://doi.org/10.1038/s41559-019-1049-1

Harvey, H. R., & McManus, G. B. (1991). Marine ciliates as a widespread source of tetrahymanol and hopan-3β-ol in sediments. *Geochimica et Cosmochimica Acta*, *55*(11), 3387–3390. https://doi.org/10.1016/0016-7037(91)90496-R

Hofheinz, W., & Oesterhelt, G. (1979). 24-isopropylcholesterol and 22-Dehydro-24-isopropylcholesterol, novel sterols from a sponge. *Helvetica Chimica Acta*, *62*(4), 1307–1309. https://doi.org/10.1002/hlca.19790620443

Kaneda, T. (1991). Iso- and anteiso-fatty acids in bacteria: Biosynthesis, function, and taxonomic significance. *Microbiological Reviews*, *55*(2), 288–302.

Kelly, A. E., Love, G. D., Zumberge, J. E., & Summons, R. E. (2011). Hydrocarbon biomarkers of Neoproterozoic to Lower Cambrian oils from eastern Siberia. *Organic Geochemistry*, *42*(6), 640–654. https://doi.org/10.1016/j.orggeochem.2011.03.028

Khomentovsky, V. V., & Karlova, G. A. (1993). Biostratigraphy of the Vendian-Cambrian beds and the lower Cambrian boundary in Siberia. *Geological Magazine*, *130*(1), 29–45. https://doi.org/10.1017/S0016756800023700

Killops, S. D., & Killops, V. J. (2005). *Introduction to organic geochemistry* (2nd ed.). Malden, MA: Wiley; Blackwell Publ. https://doi.org/10.1002/9781118697214

Kissin, Y. V. (1987). Catagenesis and composition of petroleum: Origin of n-alkanes and isoalkanes in petroleum crudes. *Geochimica et Cosmochimica Acta*, *51*(9), 2445–2457. https://doi.org/10.1016/0016-7037(87)90296-1

Kleemann, G., Poralla, K., Englert, G., Kjosen, H., Liaaen-Jensen, S., Neunlist, S., & Rohmer, M. (1990). Tetrahymanol from the phototrophic bacterium *Rhodopseudomonas palustris*: First report of a gammacerane triterpene from a prokaryote. *Microbiology*, *136*(12), 2551–2553. https://doi.org/10.1099/00221287-136-12-2551

Knoll, A. H., Grotzinger, J. P., Kaufman, A. J., & Kolosov, P. (1995). Integrated approaches to terminal Proterozoic stratigraphy: An example from the Olenek Uplift, northeastern Siberia. *Precambrian Research*, *73*(1–4), 251–270. https://doi.org/10.1016/0301-9268(94)00081-2

Knoll, A. H., Summons, R. E., Waldbauer, J. R., & Zumberge, J. E. (2007). The geological succession of primary producers in the oceans. In A. H. Knoll, & P. G. Falkowski (Eds.), *Evolution of primary producers in the sea* (pp. 133–163). Amsterdam, The Netherlands; Boston, MA: Elsevier Academic Press. https://doi.org/10.1016/B978-0123705181-50009-6

Knoll, A. H., Walter, M. R., Narbonne, G. M., & Christie-Blick, N. (2004). A new period for the geologic time scale. *Science*, *305*(5684), 621–622. https://doi.org/10.1126/science.1098803

Knoll, A., Walter, M., Narbonne, G., & Christie-Blick, N. (2006). The Ediacaran Period: A new addition to the geologic time scale. *Lethaia*, *39*(1), 13–30. https://doi.org/10.1080/00241160500409223

Kodner, R. B., Pearson, A., Summons, R. E., & Knoll, A. H. (2008). Sterols in red and green algae: Quantification, phylogeny, and relevance for the interpretation of geologic steranes. *Geobiology*, *6*(4), 411–420. https://doi.org/10.1111/j.1472-4669.2008.00167.x

Landing, E. (1994). Precambrian-Cambrian boundary global stratotype ratified and a new perspective of Cambrian time. *Geology*, *22*(2), 179–182. https://doi.org/10.1130/0091-7613(1994)022<0179:PCBGSR>2.3.CO;2

Lee, C. (2016). *A lipid biomarker and stable isotopic investigation of Ediacaran and modern marine microbial communities and carbon cycling*. Doctoral dissertation. UC Riverside. https://escholarship.org/uc/item/8gm644zx

Lee, C., Love, G. D., Jahnke, L. L., Kubo, M. D., & Des Marais, D. J. (2019). Early diagenetic sequestration of microbial mat lipid biomarkers through covalent binding into insoluble macromolecular organic matter (IMOM) as revealed by sequential chemolysis and catalytic hydropyrolysis. *Organic Geochemistry*, *132*, 11–22. https://doi.org/10.1016/j.orggeochem.2019.04.002

Love, G. D., Grosjean, E., Stalvies, C., Fike, D. A., Grotzinger, J. P., Bradley, A. S., … Bowring, S. A. (2009). Fossil steroids record the appearance of Demospongiae during the Cryogenian period. *Nature*, *457*(7230), 718–721. https://doi.org/10.1038/nature07673

Love, G. D., Stalvies, C., Grosjean, E., Meredith, W., & Snape, C. E. (2008). Analysis of molecular biomarkers covalently bound within Neoproterozoic sedimentary kerogen. *The Paleontological Society Papers*, *14*, 67–83. https://doi.org/10.1017/S1089332600001613

Love, G. D., Zumberge, J. A., Cárdenas, P., Sperling, E. A., Rohrssen, M., Grosjean, E., … Summons, R. E. (2020). Sources of C_{30} steroid biomarkers in Neoproterozoic-Cambrian rocks and oils. *Nature Ecology and Evolution*, *4*(1), 34–36. https://doi.org/10.1038/s41559-019-1048-2

Mackenzie, A. S., Patience, R. L., Maxwell, J. R., Vandenbroucke, M., & Durand, B. (1980). Molecular parameters of maturation in the Toarcian shales, Paris Basin, France—I. Changes in the configurations of acyclic isoprenoid alkanes, steranes and triterpanes. *Geochimica et Cosmochimica Acta*, *44*(11), 1709–1721. https://doi.org/10.1016/0016-7037(80)90222-7

Markov, G., Rogov, V., Karlova, G., & Grazhdankin, D. (2019). Taphonomic bias in Cloudina distribution data from Siberia. *Estudios Geológicos*, *75*(2), 10–3989. https://doi.org/10.3989/egeol.43590.559

McCaffrey, M. A., Moldowan, J. M., Lipton, P. A., Summons, R. E., Peters, K. E., Jeganathan, A., & Watt, D. S. (1994). Paleoenvironmental implications of novel C30 steranes in Precambrian to Cenozoic age petroleum and bitumen. *Geochimica et Cosmochimica Acta*, *58*(1), 529–532. https://doi.org/10.1016/0016-7037(94)90481-2

Mello, M. R., Telnæs, N., Gaglianone, P. C., Chicarelli, M. I., Brassell, S. C., & Maxwell, J. R. (1988). Organic geochemical characterisation of depositional palaeoenvironments of source rocks and oils in Brazilian marginal basins. *Organic Geochemistry*, *13*(1–3), 31–45. https://doi.org/10.1016/0146-6380(88)90023-X

Melnik, D. S., Parfenova, T. M., Grazhdankin, D. V., & Rogov, V. I. (2019). Deposition of the Khatyspyt Facies, Northeastern Siberia. In *Proceedings, 29th International Meeting on Organic Geochemistry*. BV Netherlands: EAGE Publications. https://doi.org/10.3997/2214-4609.201902903

Mißbach, H., Duda, J.-P., Lünsdorf, N. K., Schmidt, B. C., & Thiel, V. (2016). Testing the preservation of biomarkers during experimental maturation of an immature kerogen. *International Journal of Astrobiology*, *15*(3), 165–175. https://doi.org/10.1017/S1473550416000069

Moldowan, J. M., Fago, F. J., Carlson, R. M., Young, D. C., an Duvne, G., Clardy, J., … Watt, D. S. (1991). Rearranged hopanes in sediments and petroleum. *Geochimica et Cosmochimica Acta*, *55*(11), 3333–3353. https://doi.org/10.1016/0016-7037(91)90492-N

Moldowan, J. M., & McCaffrey, M. A. (1995). A novel microbial hydrocarbon degradation pathway revealed by hopane demethylation in a petroleum reservoir. *Geochimica et Cosmochimica Acta*, *59*(9), 1891–1894. https://doi.org/10.1016/0016-7037(95)00072-8

Moldowan, J. M., Seifert, W. K., & Gallegos, E. J. (1985). Relationship between petroleum composition and depositional environment of petroleum source rocks. *AAPG Bulletin*, *69*(8), 1255–1268. https://doi.org/10.1306/AD462BC8-16F7-11D7-8645000102C1865D

Moldowan, J. M., Sundararaman, P., & Schoell, M. (1986). Sensitivity of biomarker properties to depositional environment and/or source input in the Lower Toarcian of SW-Germany. *Organic Geochemistry*, *10*(4–6), 915–926. https://doi.org/10.1016/S0146-6380(86)80029-8

Nagovitsin, K. E., Rogov, V. I., Marusin, V. V., Karlova, G. A., Kolesnikov, A. V., Bykova, N. V., & Grazhdankin, D. V. (2015). Revised neoproterozoic and terreneuvian stratigraphy of the lena-anabar basin and north-western slope of the olenek uplift, siberian platform. *Precambrian Research*, *270*, 226–245. https://doi.org/10.1016/j.precamres.2015.09.012

Narbonne, G. M. (2005). The Ediacara biota: Neoproterozoic origin of animals and their ecosystems. *Annual Review of Earth and Planetary Sciences*, *33*(1), 421–442. https://doi.org/10.1146/annurev.earth.33.092203.122519

Narbonne, G. M., Xiao, S., Shields, G. A., & Gehling, J. G. (2012). The Ediacaran period. *The Geologic Time Scale*, *1*, 413–435.

Nettersheim, B. J., Brocks, J. J., Schwelm, A., Hope, J. M., Not, F., Lomas, M., … Pawlowski, J. (2019). Putative sponge biomarkers in unicellular Rhizaria question an early rise of animals. *Nature Ecology and Evolution*, *3*(4), 577–581. https://doi.org/10.1038/s41559-019-0806-5

Ourisson, G., Albrecht, P., & Rohmer, M. (1979). The hopanoids: Palaeochemistry and biochemistry of a group of natural products. *Pure and Applied Chemistry*, *51*(4), 709–729. https://doi.org/10.1351/pac197951040709

Pawlowska, M. M., Butterfield, N. J., & Brocks, J. J. (2013). Lipid taphonomy in the Proterozoic and the effect of microbial mats on biomarker preservation. *Geology*, *41*(2), 103–106. https://doi.org/10.1130/G33525.1

Peakman, T. M., ten Haven, H. L., Rechka, J. R., de Leeuw, J. W., & Maxwell, J. R. (1989). Occurrence of (20R)-and (20S)-Δ8 (14) and Δ14 5α (H)-sterenes and the origin of 5α (H), 14β (H), 17β (H)-steranes in an immature sediment. *Geochimica et Cosmochimica Acta*, *53*(8), 2001–2009. https://doi.org/10.1016/0016-7037(89)90320-7

Pehr, K., Love, G. D., Kuznetsov, A., Podkovyrov, V., Junium, C. A. K., Shumlyanskyy, L., … Bekker, A. (2018). Ediacara biota flourished in oligotrophic and bacterially dominated marine environments across Baltica. *Nature Communications*, *9*(1), 1807. https://doi.org/10.1038/s41467-018-04195-8

Pelechaty, S. M., Grotzinger, J. P., Kashirtsev, V. A., & Zhernovsky, V. P. (1996). Chemostratigraphic and sequence stratigraphic constraints on Vendian-Cambrian basin dynamics, northeast siberian craton. *The Journal of Geology*, *104*(5), 543–563. https://doi.org/10.1086/629851

Pelechaty, S. M., Kaufman, A. J., & Grotzinger, J. P. (1996). Evaluation of $\delta^{13}C$ chemostratigraphy for intrabasinal correlation: Vendian strata of northeast Siberia. *Geological Society of America Bulletin*, *108*(8), 992–1003. https://doi.org/10.1130/0016-7606(1996)108<0992:EOCCFI>2.3.CO;2

Peters, K. E. (1986). Guidelines for evaluating petroleum source rock using programmed pyrolysis. *AAPG Bulletin*, *70*(3), 318–329. https://doi.org/10.1306/94885688-1704-11D7-8645000102C1865D

Peters, K. E., & Cassa, M. R. (1994). Applied source rock Geochemistry: Chapter 5: Part II. Essential elements. In: K. E. Peters, M. R. Cassa, L. B. Magoon, & W. G. Dow (Eds.), *The petroleum system—From source to trap*. *AAPG Memoir*, *60*, 93–120.

Peters, K. E., Clark, M. E., Gupta, U. D., McCaffrey, M. A., & Lee, C. Y. (1995). Recognition of an Infracambrian source rock based on biomarkers in the Baghewala-1 oil, India. *AAPG Bulletin*, *79*(10), 1481–1494.

Peters, K. E., & Moldowan, J. M. (1991). Effects of source, thermal maturity, and biodegradation on the distribution and isomerization of homohopanes in petroleum. *Organic Geochemistry*, *17*(1), 47–61. https://doi.org/10.1016/0146-6380(91)90039-M

Peters, K. E., Moldowan, J. M., McCaffrey, M. A., & Fago, F. J. (1996). Selective biodegradation of extended hopanes to 25-norhopanes in petroleum reservoirs. *Insights from Molecular Mechanics*. *Organic Geochemistry*, *24*(8–9), 765–783. https://doi.org/10.1016/S0146-6380(96)00086-1

Peters, K. E., Walters, C. C., & Moldowan, J. M. (2005). *The biomarker guide 2: Biomarkers and isotopes in petroleum systems and earth history (Second edition, digitally printed version)*. Cambridge, UK: Cambridge University Press. https://doi.org/10.1017/CBO9781107326040

Philp, R. P. (1985). Biological markers in fossil fuel production. *Mass Spectrometry Reviews*, *4*(1), 1–54. https://doi.org/10.1002/mas.1280040102

Pu, F., Yaorong, Q., & Baisheng, Z. (1991). Characteristics of biomarkers in the Recent sediment from Qinghai Lake, northwest China. *Journal of Southeast Asian Earth Sciences*, *5*(1–4), 113–128. https://doi.org/10.1016/0743-9547(91)90019-T

Radke, M., & Welte, D. H. (1983). The Methylphenanthrene Index (MPI): A Maturity Parameter based on Aromatic Hydrocarbons. In *Advances in Organic Geochemistry 1981: 10th International Meeting on Organic Geochemistry, Bergen, September 1981, Proceedings*. M. Bjorøy, & European Association of Organic Geochemists (pp. 504–512). Chichester, UK: Wiley.

Radke, M., Welte, D. H., & Willsch, H. (1982). Geochemical study on a well in the Western Canada Basin: Relation of the aromatic distribution pattern to maturity of organic matter. *Geochimica et Cosmochimica Acta*, *46*(1), 1–10. https://doi.org/10.1016/0016-7037(82)90285-X

Radke, M., Welte, D. H., & Willsch, H. (1986). Maturity parameters based on aromatic hydrocarbons: Influence of the organic matter type. *Organic Geochemistry*, *10*(1–3), 51–63. https://doi.org/10.1016/0146-6380(86)90008-2

Rashby, S. E., Sessions, A. L., Summons, R. E., & Newman, D. K. (2007). Biosynthesis of 2-methylbacteriohopanepolyols by an anoxygenic phototroph. *Proceedings of the National Academy of Sciences of the United States of America*, *104*(38), 15099–15104. https://doi.org/10.1073/pnas.0704912104

Requejo, A. G., Hieshima, G. B., Hsu, C. S., McDonald, T. J., & Sassen, R. (1997). Short-chain (C21 and C22) diasteranes in petroleum and source rocks as indicators of maturity and depositional environment. *Geochimica et Cosmochimica Acta*, *61*(13), 2653–2667. https://doi.org/10.1016/S0016-7037(97)00106-3

Rogov, V. I., Karlova, G. A., Marusin, V. V., Kochnev, B. B., Nagovitsin, K. E., & Grazhdankin, D. V. (2015). Duration of the first biozone in the Siberian hypostratotype of the Vendian. *Russian Geology and Geophysics*, *56*(4), 573–583. https://doi.org/10.1016/j.rgg.2015.03.016

Rogov, V., Marusin, V., Bykova, N., Goy, Y., Nagovitsin, K., Kochnev, B., … Grazhdankin, D. (2012). The oldest evidence of bioturbation on Earth. *Geology*, *40*(5), 395–398. https://doi.org/10.1130/G32807.1

Rohmer, M., Bouvier-Navé, P., & Ourisson, G. (1984). Distribution of hopanoid triterpenes in prokaryotes. *Microbiology*, *130*(5), 1137–1150. https://doi.org/10.1099/00221287-130-5-1137

Rubinstein, I., & Strausz, O. P. (1979). Geochemistry of the thiourea adduct fraction from an Alberta petroleum. *Geochimica et Cosmochimica Acta*, *43*(8), 1387–1392. https://doi.org/10.1016/0016-7037(79)90129-7

Schröder, S., & Grotzinger, J. P. (2007). Evidence for anoxia at the Ediacaran-Cambrian boundary: The record of redox-sensitive trace elements and rare earth elements in Oman. *Journal of the Geological Society*, *164*(1), 175–187. https://doi.org/10.1144/0016-76492005-022

Seifert, W. K., & Moldowan, J. M. (1978). Applications of steranes, terpanes and monoaromatics to the maturation, migration and source of crude oils. *Geochimica et Cosmochimica Acta*, *42*(1), 77–95. https://doi.org/10.1016/0016-7037(78)90219-3

Seifert, W. K., & Moldowan, J. M. (1979). The effect of biodegradation on steranes and terpanes in crude oils. *Geochimica et Cosmochimica Acta*, *43*(1), 111–126. https://doi.org/10.1016/0016-7037(79)90051-6

Seifert, W. K., & Moldowan, J. M. (1980). The effect of thermal stress on source-rock quality as measured by hopane stereochemistry. *Physics and Chemistry of the Earth*, *12*, 229–237. https://doi.org/10.1016/0079-1946(79)90107-1

Seifert, W. K., & Moldowan, J. M. (1986). Use of biological markers in petroleum exploration. *Methods in Geochemistry and Geophysics*, *24*, 261–290.

Seilacher, A. (1970). Begriff und Bedeutung der Fossil-Lagerstätten. *Neues Jahrbuch Für Geologie und Paläontologie*, *Monatshefte*, *1*, 34–39.

Seilacher, A., & Pflüger, F. (1994). From biomats to benthic agriculture: A biohistortic revolution. In W. E. Krumbein, D. M. Paterson, L. J. Stal (Eds.), *Biostabilization of sediments* (pp. 97–105). Oldenburg, Germany: Universität Oldenburg.

Shen, Y., Thiel, V., Duda, J. P., & Reitner, J. (2018). Tracing the fate of steroids through a hypersaline microbial mat (Kiritimati, Kiribati/Central Pacific). *Geobiology*, *16*(3), 307–318. https://doi.org/10.1111/gbi.12279

Shiea, J., Brassell, S. C., & Ward, D. M. (1990). Mid-chain branched mono-and dimethyl alkanes in hot spring cyanobacterial mats: A direct biogenic source for branched alkanes in ancient sediments? *Organic Geochemistry*, *15*(3), 223–231. https://doi.org/10.1016/0146-6380(90)90001-G

Sinninghe Damsté, J. S., Kenig, F., Koopmans, M. P., Koster, J., Schouten, S., Hayes, J. M., & de Leeuw, J. W. (1995). Evidence for gammacerane as an indicator of water column stratification. *Geochimica et Cosmochimica Acta*, *59*(9), 1895–1900. https://doi.org/10.1016/0016-7037(95)00073-9

Sokolov, B. S., & Fedonkin, M. A. (1984). The Vendian as the terminal system of the Precambrian. *Episodes*, *7*(1), 12–19.

Steiner, M., Erdtmann, B. D., & Chen, J. Y. (1992). Preliminary assessment of new Late Sinian (Late Proterozoic) large siphonous and filamentous "megaalgae" from eastern Wulingshan, north-central Hunan, China. *Berliner Geowissenschaftliche Abhandlungen (E)*, *3*, 305–319.

Summons, R. E., Bradley, A. S., Jahnke, L. L., & Waldbauer, J. R. (2006). Steroids, triterpenoids and molecular oxygen. *Philosophical Transactions of the Royal Society B: Biological Sciences*, *361*(1470), 951–968. https://doi.org/10.1098/rstb.2006.1837

Summons, R. E., & Capon, R. J. (1988). Fossil steranes with unprecedented methylation in ring-A. *Geochimica et Cosmochimica Acta*, *52*(11), 2733–2736. https://doi.org/10.1016/0016-7037(88)90042-7

Summons, R. E., & Capon, R. J. (1991). Identification and significance of 3β-ethyl steranes in sediments and petroleum. *Geochimica et Cosmochimica Acta*, *55*(8), 2391–2395. https://doi.org/10.1016/0016-7037(91)90116-M

Summons, R. E., & Powell, T. G. (1987). Identification of aryl isoprenoids in source rocks and crude oils: Biological markers for the green sulphur bacteria. *Geochimica et Cosmochimica Acta*, *51*(3), 557–566. https://doi.org/10.1016/0016-7037(87)90069-X

Summons, R. E., & Powell, T. G. (1992). Hydrocarbon composition of the Late Proterozoic oils of the Siberian Platform: Implications for the depositional environment of source rocks. In M. Schidlowski, S. Golubic, M. M. Kimberley, D. M. McKirdy, & P. A. Trudinger (Eds.), *Early organic evolution* (pp. 296–307). Berlin, Heidelberg: Springer.

Summons, R. E., & Walter, M. R. (1990). Molecular fossils and microfossils of prokaryotes and protists from Proterozoic sediments. *American Journal of Science*, *290*(A), 212–244.

Suzuki, K. I., Saito, K., Kawaguchi, A., Okuda, S., & Komagata, K. (1981). Occurrence of ω-cyclohexyl fatty acids in *Curtobacteriui pusillum* strains. *The Journal of General and Applied Microbiology*, *27*(3), 261–266. https://doi.org/10.2323/jgam.27.261

ten Haven, H. L., de Leeuw, J. W., Damsté, J. S., Schenck, P. A., Palmer, S. E., & Zumberge, J. E. (1988). Application of biological markers in the recognition of palaeohypersaline environments. *Geological Society, London, Special Publications*, *40*(1), 123–130. https://doi.org/10.1144/GSL.SP.1988.040.01.11

ten Haven, H. L., de Leeuw, J. W., Peakman, T. M., & Maxwell, J. R. (1986). Anomalies in steroid and hopanoid maturity indices. *Geochimica et Cosmochimica Acta*, *50*(5), 853–855. https://doi.org/10.1016/0016-7037(86)90361-3

ten Haven, H. L., de Leeuw, J. W., & Schenck, P. A. (1985). Organic geochemical studies of a Messinian evaporitic basin, northern Apennines (Italy) I: Hydrocarbon biological markers for a hypersaline environment. *Geochimica et Cosmochimica Acta*, *49*(10), 2181–2191. https://doi.org/10.1016/0016-7037(85)90075-4

ten Haven, H. L., Rohmer, M., Rullkötter, J., & Bisseret, P. (1989). Tetrahymanol, the most likely precursor of gammacerane, occurs ubiquitously in marine sediments. *Geochimica et Cosmochimica Acta*, *53*(11), 3073–3079. https://doi.org/10.1016/0016-7037(89)90186-5

Tissot, B. P., & Welte, D. H. (1984). *Petroleum formation and occurrence (Second Revised and Enlarged Edition)*. Berlin, Heidelberg, s.l.: Springer Berlin Heidelberg. https://doi.org/10.1007/978-3-642-87813-8

Vodanjuk, S. A. (1989). Non-skeletal fossil Metazoa from the Khatyspyt formation of the Olenek Uplift. In V. V. Khomentovsky, J. K. Sovetov, & IGG SO AN SSSR (pp. 61–74). *Late Precambrian and Early Palaeozoic of Siberia. Urgent Stratigraphic Problems*. Novosibirsk, (in Russian).

Volkman, J. K. (1986). A review of sterol markers for marine and terrigenous organic matter. *Organic Geochemistry*, *9*(2), 83–99. https://doi.org/10.1016/0146-6380(86)90089-6

Volkman, J. (2003). Sterols in microorganisms. *Applied Microbiology and Biotechnology*, *60*(5), 495–506. https://doi.org/10.1007/s00253-002-1172-8

Wei, J. H., Yin, X., & Welander, P. V. (2016). Sterol synthesis in diverse bacteria. *Frontiers in Microbiology*, *7*, 990. https://doi.org/10.3389/fmicb.2016.00990

Welander, P. V., Coleman, M. L., Sessions, A. L., Summons, R. E., & Newman, D. K. (2010). Identification of a methylase required for 2-methylhopanoid production and implications for the interpretation of sedimentary hopanes. *Proceedings of the National Academy of Sciences of the United States of America*, *107*(19), 8537–8542. https://doi.org/10.1073/pnas.0912949107

Welander, P. V., Hunter, R. C., Zhang, L., Sessions, A. L., Summons, R. E., & Newman, D. K. (2009). Hopanoids play a role in membrane integrity and pH homeostasis in *Rhodopseudomonas palustris* TIE-1. *Journal of Bacteriology*, *191*(19), 6145–6156. https://doi.org/10.1128/JB.00460-09

Wingert, W. S., & Pomerantz, M. (1986). Structure and significance of some twenty-one and twenty-two carbon petroleum steranes. *Geochimica et Cosmochimica Acta*, *50*(12), 2763–2769. https://doi.org/10.1016/0016-7037(86)90225-5

Xiao, Q., She, Z., Wang, G., Li, Y., Ouyang, G., Cao, K., … Du, Y. (2020). Terminal Ediacaran carbonate tempestites in the eastern Yangtze Gorges area, South China. *Palaeogeography, Palaeoclimatology, Palaeoecology*, *547*, 109681. https://doi.org/10.1016/j.palaeo.2020.109681

Xiao, S., Chen, Z., Zhou, C., & Yuan, X. (2019). Surfing in and on microbial mats: Oxygen-related behavior of a terminal Ediacaran bilaterian animal. *Geology*, *47*(11), 1054–1058. https://doi.org/10.1130/G46474.1

Xiao, S., & Laflamme, M. (2009). On the eve of animal radiation: Phylogeny, ecology and evolution of the Ediacara biota. *Trends in Ecology and Evolution*, *24*(1), 31–40. https://doi.org/10.1016/j.tree.2008.07.015

Yakshin, M. S. (1987). Vendian of the olenek uplift. In V. V. Khomentovsky, V. Y. Shenfil, & IGG SO AN SSSR. *Late Precambrian and Early Palaeozoic of Siberia. The Siberian Platform and the Adjacent Southern Folded Belt* (pp. 18–30). Novosibirsk (in Russian).

Zumberge, J. A. (2019). *A lipid biomarker investigation tracking the evolution of the neoproterozoic marine biosphere and the rise of eukaryotes*. Doctoral dissertation. UC Riverside: https://escholarship.org/uc/item/86p25344

Zumberge, J. A., Cárdenas, P., Duda, J. P., Sperling, E. A., & Love, G. D. (2019). Patterns of steroid synthesis in modern demosponges and the identification of new sterane biomarker targets. In *29th International Meeting on Organic Geochemistry* (Vol. *2019*, pp. 1–2). European Association of Geoscientists & Engineers.

Zumberge, J. A., Love, G. D., Cárdenas, P., Sperling, E. A., Gunasekera, S., Rohrssen, M., … Summons, R. E. (2018). Demosponge steroid biomarker 26-methylstigmastane provides evidence for Neoproterozoic animals. *Nature Ecology and Evolution*, *2*(11), 1709–1714. https://doi.org/10.1038/s41559-018-0676-2

SUPPORTING INFORMATION

Additional supporting information may be found online in the Supporting Information section.

How to cite this article: Duda J-P, Love GD, Rogov VI, Melnik DS, Blumenberg M, Grazhdankin DV. Understanding the geobiology of the terminal Ediacaran Khatyspyt Lagerstätte (Arctic Siberia, Russia). *Geobiology*. 2020;00:1–20. https://doi.org/10.1111/gbi.12412